

Chapman University

Chapman University Digital Commons

Pharmaceutical Sciences (MS) Theses

Dissertations and Theses

Spring 5-2022

Content and Activity of Cytochrome P450 3A in Rat Brain Microsomes and Mitochondria

Nouf Alshammari

Chapman University, nalshammari@chapman.edu

Follow this and additional works at: [https://digitalcommons.chapman.edu/
pharmaceutical_sciences_theses](https://digitalcommons.chapman.edu/pharmaceutical_sciences_theses)



Part of the [Other Pharmacy and Pharmaceutical Sciences Commons](#)

Recommended Citation

Alshammari, N. *Content and Activity of Cytochrome P450 3A in Rat Brain Microsomes and Mitochondria*. [master's thesis]. Irvine, CA: Chapman University; 2022. <https://doi.org/10.36837/chapman.000364>

This Thesis is brought to you for free and open access by the Dissertations and Theses at Chapman University Digital Commons. It has been accepted for inclusion in Pharmaceutical Sciences (MS) Theses by an authorized administrator of Chapman University Digital Commons. For more information, please contact laughtin@chapman.edu.

Content and Activity of Cytochrome P450 3A in Rat Brain

Microsomes and Mitochondria

A Thesis by

Nouf Alshammari

Chapman University

Irvine, CA

School of Pharmacy

Submitted in partial fulfillment of the requirements for the degree of

Master in Pharmaceutical Sciences

May 2022

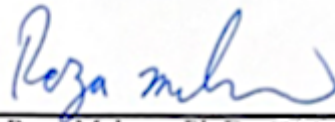
Committee in charge:

Reza Mehvar, Ph.D., Chair

Ajay Sharma, Ph.D.

Aftab Ahmed, Ph.D.

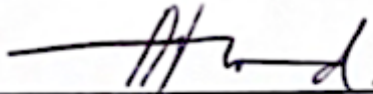
The thesis of Nouf Alshammari is approved.



Reza Mehvar, Ph.D., Chair



Ajay Sharma, Ph.D.



Aftab Ahmed, Ph.D.

May 2022

**Content and Activity of Cytochrome P450 3A in Rat Brain
Microsomes and Mitochondria**

Copyright © 2022

by Nouf Alshammari

ACKNOWLEDGEMENTS

First and foremost, I would like to express my sincere thanks to my supervisor Dr. Reza Mehvar, for his guidance and commitment throughout this project. His advice and unwavering support have been invaluable. I am also extremely grateful to the members of my thesis committee: Dr. Ajay Sharma and Dr. Aftab Ahmed, whose support and advice I have valued highly. I wish to thank all of the past and present group members of the pharmacokinetics lab: Dr. Devaraj Venkatapura Chandnra and Dr. FNU Mamunur Rashid, for their help in the method development in the analytical instrumentation. A great thanks is owed to my colleague: Nouf Alwadei for her friendship. Thanks, must also go to Saudi Arabian Cultural Mission (SACM) for the funding. On a personal level, I would like to thank my husband and best friend, Salman Alshammari, who has been a constant source of support and encouragement during the challenges of graduate school and life. I also wish to extend my heartfelt thanks to my son, who inspired me to continue and complete my graduate education. Last but not least, I would like to thank my family for their love and support.

ABSTRACT

Content and Activity of Cytochrome P450 3A in Rat Brain Microsomes and Mitochondria.

by: Nouf Alshammari

The potential contribution of CYP3A in brain microsomes and mitochondria is crucial to designing appropriate therapeutic strategies and preventing toxicities. Until recently, there has been limited data reported in the literature with respect to CYP3A activity and its expression in the brain tissue. The reason for this limitation is most likely the relatively low level of CYP3A in the brain tissue. To this end, the primary purpose of this study is to develop a CYP3A functional assay in rat brain mitochondria and microsomes to determine the Michaelis-Menten kinetics of the formation of CYP3A-mediated hydroxylated metabolites of midazolam by UPLC-MS/MS. We also aim to analyze the protein levels of CYP3A in the rat brain mitochondria and microsomes by Western blot analysis.

Microsome and mitochondria were prepared using different centrifugation methods, followed by purification of the crude mitochondrial fractions using the Percoll density gradient method. The purity of the fractions was determined by Western blot analysis of the microsomal (calreticulin) and mitochondrial (VDAC) markers. Different concentrations of midazolam were incubated with rat brain microsomes and mitochondria in a side-by-side comparison over a period of 10 minutes.

The method was developed and optimized to determine the Michaelis-Menten kinetics of MDZ 1'- and 4-hydroxylase activities in rat brain microsomes and mitochondria (n=8). For 4-hydroxymidazolam, brain mitochondria had 2.5-fold higher maximum velocity and 5-fold higher MM constant compared to microsomes. For 1'-hydroxymidazolam, mitochondria had 9-fold higher maximum velocity and 153-fold higher MM constant compared to microsomes. Consistent with the higher Vmax of the metabolites in the mitochondrial fractions, the Western blot analysis showed higher band intensities related to CYP3A2 in the brain mitochondria, when compared with the brain microsomes. Our in vitro study indicates that in the brain the content and activity of CYP3A in the mitochondria are higher than those in the microsomes, an observation which is opposite of the pattern reported in the liver. The local metabolism of CYP3A substrates in the brain microsomes and mitochondria may have significant ramifications for the effectiveness or toxicity of the centrally-acting drugs that are CYP3A substrates.

TABLE OF CONTENT

ACKNOWLEDGEMENTS	IV
ABSTRACT	V
LIST OF TABLES.....	VIII
LIST OF FIGURES.....	IIX
CHAPTER 1.....	1
Introduction.....	1
CHAPTER 2.....	25
Methodology.....	25
CHAPTER 3.....	37
Result	37
CHAPTER 4.....	52
Discussion.....	52
CHAPTER 5.....	56
Conclusion.....	56
BIBLIOGRAPHY.....	57

LIST OF TABLES

TABLE 1 CYTOCHROME P450 FAMILIES AND SUBFAMILIES IN RATS AND HUMANS.	4
TABLE 2 MICROSOMAL AND MITOCHONDRIAL P450 ELECTRON TRANSFER SYSTEMS	7
TABLE 3 GENERAL CHARACTERISTICS OF CYP1-3 IN HUMAN	11
TABLE 4 LC/MS/MS SETTING FOR CYP3A.....	30
TABLE 5 4-OH MDZ SLOPE AND COEFFICIENT OF R2 IN MICROSONE AND MITOCHONDRIA.	43
TABLE 6 1'-OH MDZ SLOPE AND COEFFICIENT OF R2 IN MICROSONE AND MITOCHONDRIA.	43
TABLE 7 INTRA-RUN PRECISION AND ACCURACY OF 4-HYDROXYMIDAZOLAM AND 1'- HYDROXYMIDAZOLAM QUALITY CONTROL SAMPLES IN RAT BRAIN MITOCHONDRIA.	46
TABLE 8 INTRA-RUN PRECISION AND ACCURACY OF 4-HYDROXYMIDAZOLAM AND 1'- HYDROXYMIDAZOLAM QUALITY CONTROL SAMPLES IN RAT BRAIN MICROSONE.	47
TABLE 9 INTER-RUN PRECISION AND ACCURACY OF 4-HYDROXYMIDAZOLAM AND 1'- HYDROXYMIDAZOLAM QUALITY CONTROL SAMPLES IN RAT BRAIN MITOCHONDRIA.	48
TABLE 10 INTER-RUN PRECISION AND ACCURACY OF 4-HYDROXYMIDAZOLAM AND 1'- HYDROXYMIDAZOLAM QUALITY CONTROL SAMPLES IN RAT BRAIN MICROSONE.	49
TABLE 11 MAXIMUM VELOCITY (V _{MAX}) AND MICHAELIS-MENTEN CONSTANT (K _M) VALUES (MEAN ± SD, N = 8 BRAINS) OF 1'-OH MIDAZOLAM METABOLITES IN RAT BRAIN MICROSONES AND MITOCHONDRIA.....	50
TABLE 12 MAXIMUM VELOCITY (V _{MAX}) AND MICHAELIS-MENTEN CONSTANT (K _M) VALUES (MEAN ± SD, N = 8 BRAINS) OF 4-OH MIDAZOLAM METABOLITES IN RAT BRAIN MICROSONES AND MITOCHONDRIA.....	51

LIST OF FIGURES

FIGURE 1 BIOTRANSFORMATION PATHWAYS: PHASE I AND PHASE II.....	2
FIGURE 2 CYTOCHROME P450 ENZYMES IN FAMILIES 1 – 3	3
FIGURE 3 AN EXAMPLE OF THE NOMENCLATURE OF THE CYTOCHROME P450 ENZYMES (WIJNEN ET AL., 2007).....	3
FIGURE 4 THREE-DIMENSIONAL STRUCTURE OF CYP2C5 ENZYME (THOMAS M., 2011).....	6
FIGURE 5 INNER MITOCHONDRIA MEMBRANE AND ENDOPLASMIC RETICULUM MEMBRANE.....	8
FIGURE 6 CONTRIBUTION OF CYP450 IN DRUG METABOLISM.	11
FIGURE 7 CHEMICAL STRUCTURE OF MIDAZOLAM AND ITS MAJOR METABOLITE.	20
FIGURE 8 PREPARATION OF MICROSOME AND MITOCHONDRIA.....	27
FIGURE 9 IMMUNOBLOT ANALYSIS OF VDAC1, AS A MITOCHONDRIAL MARKER. STATISTICAL ANALYSIS IS BASED ON PAIRED T TEST. ****P <0.0001	38
FIGURE 10 WESTERN BLOT ANALYSIS OF VDAC IN EIGHT RAT BRAINS (MIC=MICROSOME, PM=PURIFIED MITOCHONDRIA).....	38
FIGURE 11 IMMUNOBLOT ANALYSIS OF CALRETICULIN AS A MICROSOMAL MARKER. STATISTICAL ANALYSIS IS BASED ON PAIRED T TEST. ****P <0.0001.....	39
FIGURE 12 WESTERN BLOT ANALYSIS OF CALRETICULIN IN EIGHT RAT BRAINS (MIC=MICROSOME, PM= MITOCHONDRIA).	39
FIGURE 13 WESTERN BLOT ANALYSIS OF CYP3A2 IN EIGHT INDEPENDENT BRAIN SAMPLES. STATISTICAL ANALYSIS IS BASED ON PAIRED T TEST. ****P <0.0001.....	40

FIGURE 14 WESTERN BLOT ANALYSIS IN EIGHT RAT BRAINS (MIC=MICROSOME, PM= MITOCHONDRIA).....	41
FIGURE 15 CALIBRATION CURVE OF 1'- AND 4- OH MDZ, ONE SET CONTAINING RAT BRAIN MICROSOME (0.25MG/ML) AND OTHER SET CONTAINING RAT BRAIN MITOCHONDRIA (0.25MG/ML).....	42
FIGURE 16 REPRESENTATIVE CHROMATOGRAMS OF 1-HYDROXYMIDAZOLAM (A, B AND C) AND 4-HYDROXYMIDAZOLAM (D, E AND F) GENERATED FROM RAT BRAIN MITOCHONDRIA IN BLANK, 1, OR 100 (NM) OF 4-HYDROXYMIDAZOLAM AND 1-HYDROXYMIDAZOLAM.	44
FIGURE 17 REPRESENTATIVE CHROMATOGRAMS OF 1-HYDROXYMIDAZOLAM (A, B AND C) AND 4-HYDROXYMIDAZOLAM (D, E AND F) GENERATED FROM RAT BRAIN MICROSOME IN BLANK, 1, OR 100 (NM) OF 4-HYDROXYMIDAZOLAM AND 1-HYDROXYMIDAZOLAM.	45
FIGURE 18 AVERAGE RATE OF 4-HYDROXYMIDAZOLAM AND 1'-HYDROXYMIDAZOLAM IN MITOCHONDRIAL AND MICROSOMAL SAMPLES VERSUS DIFFERENT CONCENTRATIONS OF MIDAZOLAM IN EIGHT BRAIN PREPARATIONS.	51

CHAPTER 1

Introduction

1.1.1 Cytochrome P450 enzyme

The human body has a unique system of enzymes that helps it eliminate various toxins. The study of CYP enzymes has increased dramatically over the last decade, owing to their essential role in response to therapeutic drugs and drug toxicity. Cytochrome P450 (CYP) enzymes are a superfamily of heme-containing monooxygenases (mixed-function oxidases), which catalyzes a variety of reactions involved in the metabolism of substances and the biosynthesis of cholesterol, steroids, and other lipids (Nelson, 2005). Because most medications are extremely lipid soluble and nonpolar and hence difficult for the kidney to remove, the majority of lipophilic compounds are transformed to much more polar/hydrophilic molecules that can be eliminated in the urine (Donato and Castell, 2003). This conversion occurs via a process known as biotransformation, which converts lipophilic chemicals into more hydrophilic metabolites that are more easily excreted in the urine or bile. Metabolic reactions are classified into phase I and phase II Fig. 1 (Kennedy and Tierney, 2012).

Phase I metabolic pathway is mostly oxidative in function and result in the formation of metabolites that are more polar than their precursor compounds. The purpose of phase I biotransformation is to increase the compound's polarity by exposing the functional group (e.g., -OH, -NH₂, -SH) on the medication (Jancova *et al.*, 2010). Phase II involves conjugating the drug or its metabolites to endogenous molecules, such as glucuronidation, sulfation, methylation, acetylation, glutathione, and amino acid conjugation. When compared to nonconjugated

molecules, conjugates tend to be significantly more water-soluble and, in most cases, substantially less active, therefore, less poisonous (White, 2017). They are produced by transferring a specific moiety from a coenzyme to either endogenous or exogenous substrates. The enzymes are commonly referred to as transferases, including UDP-glucuronosyltransferases, sulfotransferases, N-acetyltransferases, glutathione S-transferases, and various methyltransferases (thiopurine S-methyl transferase and catechol O-methyl transferase).

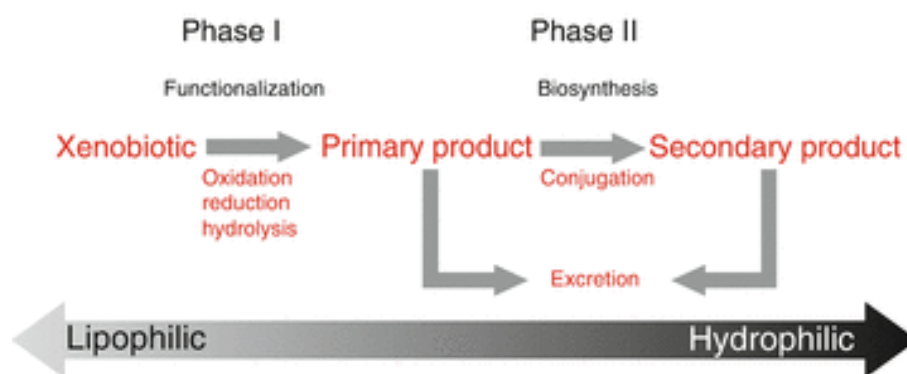


Figure 1 Biotransformation pathways: phase I and Phase II

1.1.2 The nomenclature of cytochromes P450

Based on amino acid sequence identity, enzymes are classified into families, subfamilies, and isoforms Fig. 2. An isoform is a CYP enzyme variant that derives from one specific gene. In the recent decade, extensive efforts have been made to classify CYP enzymes based on the nucleotide sequence homology of CYP genes (Nelson *et al.*, 1996). This nomenclature classification is currently widely used and allowed the CYP gene superfamily to be divided into families and subfamilies with the prefix CYP used to designate cytochrome P450 in all species (**Table 1**). All CYP families have 40% homology in amino acid sequences. A subfamily with a capital letter

contained an enzyme with 55% amino acid sequence homology (Bibi, 2008). The Isoenzyme is represented by an Arabic numeral. Figure 3 depicts an example of cytochrome P450 enzyme nomenclature.

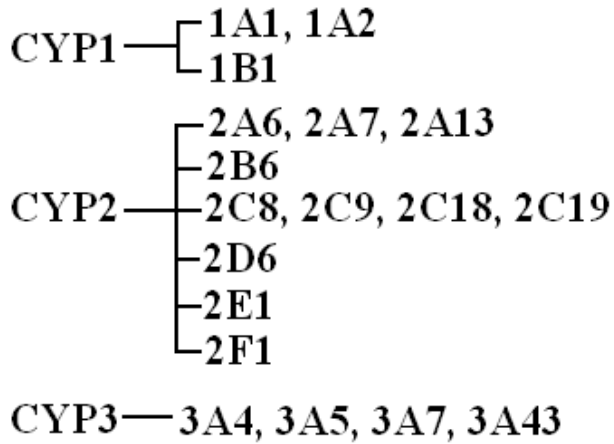


Figure 2 Cytochrome P450 enzymes in families 1 – 3

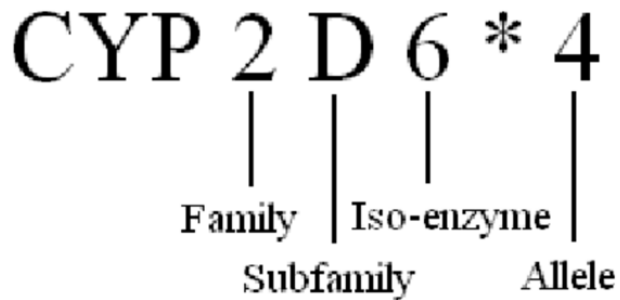


Figure 3 An example of the nomenclature of the cytochrome P450 enzymes (Wijnen et al., 2007).

Table 1 Cytochrome P450 families and subfamilies in rats and humans.

Family	Subfamily	Rat enzyme	Human enzyme
CYP1	A	1A1	1A1
		1A2	1A2
	B	1B1	1B1
CYP2	A	2A1	2A6
		2A2	2A7
		2A3	2A13
	B	2B1	2B6
		2B2	
		2B3	
		2B12	
		2B21	
	C	2C6	2C8
		2C7	2C9
		2C11	2C10
		2C12	2C18
		2C13	2C19
2C23			
2C24			

	D	2D1	2D6
		2D2	2D7P
		2D3	2D8P
		2D4	
		2D5	
		2D18	
CYP3	E	2E1	2E1
	A	3A1	3A4
		3A2	3A5
		3A9	3A7
		3A18	3A43
		3A23	

(<http://drnelson.utm.edu/CytochromeP450.html>)

OR

(<http://drnelson.uthsc.edu/human.P450.table.html>).

1.1.3 Basic features of cytochrome P450 enzymes

These enzymes are reported in the endoplasmic reticulum membranes of cells, primarily in the liver. The first report of the presence of a carbon monoxide-binding pigment in rat liver microsomes was made in 1958 (Klingenberg, 1958; Garfinkel, 2003; Cederbaum, 2015). When reduced, the pigment exhibited maximum absorbance at 450 nm during its bounding to carbon monoxide and was designated P (pigment)-450. P450 accounts for most hemoproteins detected in liver microsomes (Omura and Sato, 1964). CYP enzymes are also active in several other tissues such as the kidney, small intestine, lungs, adrenal cortex, skin, brain, testis, and placenta. With the

highest concentrations found in liver microsomes (where it plays a major role in detoxification reactions) (Omura *et al.*, 1965).

Thomas L. Poulos. (1987) discovered the three-dimensional structure of cytochrome P450. This discovery establishes the enzyme's binding sites for two molecules: one of oxygen (O₂) at its heme group and another molecule (the substrate) right above the heme group. Alpha helices and beta sheets are formed when the constituent amino acids' structures are twisted (Guengerich, 1993). The active site of cytochrome P450 is a heme-iron center. The iron is bound to the protein via a cysteine thiolate ligand. An example of the three-dimensional structure of the CYP2C5 enzyme is given in Figure 4.

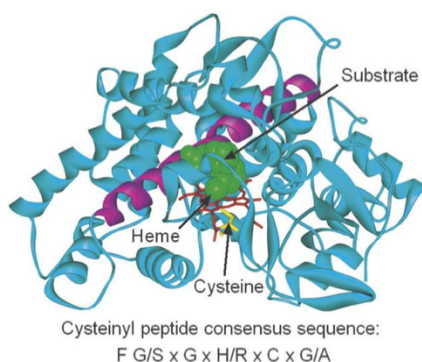


Figure 4 Three-dimensional structure of CYP2C5 enzyme (Thomas M., 2011).

1.1.4 The cytochrome P450 catalytic cycle

P450 acts as a monooxygenase by catalyzing the cleavage of molecular dioxygen and subsequent insertion of a single oxygen atom into the substrate, resulting in the formation of a water molecule. The overall catalytic process of mono-oxygenation of a substrate (RH) can be described as follows (Taniguchi *et al.*, 1984),



RH is an oxidable drug substrate, whereas ROH is the hydroxylated metabolite. NADPH is the source of the reducing equivalents involved in the transfer of electrons in oxidizing reactions. The oxygen is added to the drug to form a hydroxyl group, while the other atom of oxygen is converted to water. These reactions were discovered to occur in specific cell localization. When the cells in these tissues are homogenized, the endoplasmic reticulum within the cell membrane fragments into small vesicles known as microsomes (microsomal CYP450). P450 enzymes have also been found in mitochondria, and a novel Mitochondrial P450 was purified from adrenal cortex tissues for the first time in 1964 (Harding *et al.*, 1964) and later in other steroidogenic organs of animals (Omura, 1999). Mitochondrial P450s are integral membrane proteins that are firmly attached to the inner membrane of the cell. Their primary role is to metabolize endogenous and exogenous compounds.

1.1.5 Electron transfer to P450

Based on the nature of the electron transfer proteins, CYPs can be classified into microsomal and mitochondrial P450 systems, as summarized in Table 2. (Koymans *et al.*, 1993; Cederbaum, 2015)

Table 2 microsomal and mitochondrial P450 electron transfer systems

System	Electron transfer chain
Mitochondria	NADH + FAD + Fe ₂ S ₂ + P450
Microsome	NADPH + FAD + FMN + P450

The presence of molecular oxygen, NADPH, and a mixed-function oxidase is required for oxidation processes (cytochrome P450, NADPH- cytochrome P450 reductase). For microsomal and mitochondrial CYP450, NADPH is the preferable reductant for introducing molecular oxygen into the substrate and generating the hydroxyl group. Primary electron transport to P450 occurs via a NADPH-dependent oxidoreductase including flavoprotein (FAD and FMN). A flavoprotein is composed of a flavin group attached to an adenosine diphosphate to generate flavin adenine dinucleotide. FAD and FMN are critical cofactors for microsomal P450 heme reduction, as P450 cannot take electrons directly from NADPH. Thus, electrons are transferred from NADPH to the FAD, which then transfers electrons to FMN via CYP450 Reductase (CPR) to reduce P450's heme. CPR is required for microsomal P450 activation. Without CPR, microsomal CYP450 cannot be induced. In contrast, mitochondrial P450 utilizes two soluble proteins found within the matrix of mitochondria: Adrenodoxin (is a ferredoxin-type-iron-sulfur protein) and adrenodoxin reductase (is a FAD- containing flavoprotein). Adrenodoxin reductase transfers electrons from NADPH to FAD, thereby reducing the adrenodoxin iron-sulfur protein and, subsequently, heme iron of mitochondrial P450 (Fig. 5).

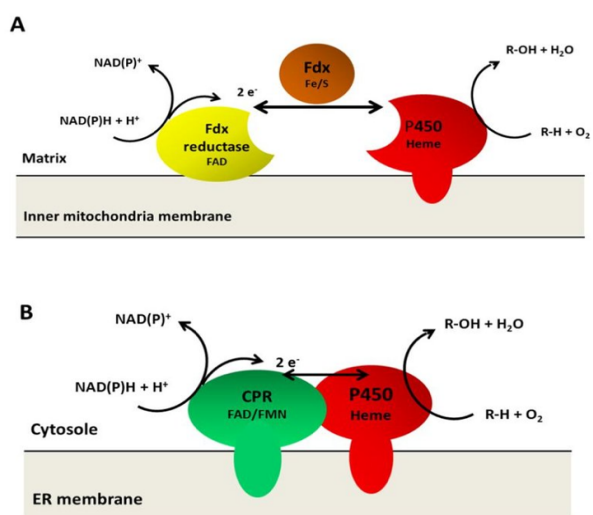


Figure 5 Inner mitochondria membrane and endoplasmic reticulum membrane

Mitochondrial CYP450(A); Adrenodoxin reductase transfers electrons from Flavin Adenine Dinucleotide to adrenodoxin (ferredoxin) and then to the heme iron of P450. Microsomal CYP450(B); CYP450 Reductase (CPR) transfers electrons to Flavin Adenine Dinucleotide, then to Flavin Mononucleotide (FMN), and then to the P450 heme iron.

https://www.researchgate.net/figure/Cytochrome-P450-redox-systems-A-The-mitochondrial-redox-chain-belongs_fig3_318861050

1.1.6 Contribution of CYP₄₅₀ in drug metabolism

Drug development is an extensive and complicated process involving the identification of the characteristics of a drug candidate to evaluate the safety and efficacy of the drug. Considerable information about the metabolism and other properties of a drug candidate is required before administering it to a human subject for the first time. Some of the characteristics generally examined for a new chemical entity is metabolic identification of metabolites, enzymes catalyzing metabolic routes and the affinity of a chemical for CYP or other enzymes. Although many CYP genes in humans and rodents play a role in the metabolism process, the metabolism of xenobiotics is mostly regulated by the first three gene families (i.e., CYP1, CYP2, and CYP3). The following table. 3 summarizes the most important features of the major drug metabolism enzymes (CYP1-3) (Ingelman-Sundberg, 2004).

The CYP3A subfamily of enzymes is the most abundant CYP that is constitutively expressed in the adult human liver, and it contributes to the elimination of the majority of all therapeutic agents now in use (Bertz and Granneman, 1997; Krishna and Shekar, 2005) Fig. 6. CYP3A is also present in many extrahepatic tissues, including the intestine, kidney, lung, adrenal gland, prostate, and brain (Finnström *et al.*, 2001; Hedlund *et al.*, 2001; Raunio *et al.*, 2005; Woodland *et al.*, 2008;

Venkatapura Chandrashekar and Mehvar, 2020). In humans, the CYP3A enzyme is found in four isoforms, namely, 3A4, 3A5, 3A7, and CYP3A43(Nelson *et al.*, 1996). Immunoblotting studies indicate that CYP3A4 is highly expressed in the liver and intestine. (Wrighton and Stevens, 1992; Paine *et al.*, 2006). It is also highly inducible by a variety of drugs and other chemicals. Its inducibility is similar to that of the drug transporter P-glycoprotein (P-gP) in the intestine. The genes are located on chromosome 7q21.1 and seem to use comparable DR4 regulatory elements for binding. *Pregnane X receptor (PXR)* is a nuclear receptor that primarily detects and upregulates the production of proteins in response to the occurrence of external toxic substances. Due to CYP3A4's broad substrate specificity and its ability for xenobiotic metabolism, as well as its co-regulation with the drug transporter P-gP, which is found in abundance in the intestine, these two components form the most significant unit for xenobiotic clearance in the body (Geick *et al.*, 2001). Hence, CYP3A4 plays a part in the metabolism of a large number of medications. CYP3A4 and CYP3A5 have identical nucleotide sequences and antibodies against CYP3A4 frequently cross-react with CYP3A5 (Belloc *et al.*, 1996). Nevertheless, CYP3A4 is more active than CYP3A5 in most CYP3A substrates and is expressed at much lower levels in the liver than CYP3A4 (Westlind-Johnsson *et al.*, 2003).

CYP3A7 is strongly expressed in the liver during the early development of a fetus, whereafter its expression declines to almost untraceable levels, and CYP3A4 levels rise to adult hepatic content (Schuetz *et al.*, 1994) (de Wildt *et al.*, 1999). CYP3A7 metabolizes many of the substances metabolized by CYP3A4 but with significant activity differences. The expression of CYP3A43 mRNA is low at about 0.1% of CYP3A4 in human liver samples. However, CYP3A43 expression is relatively higher in the brain (Agarwal *et al.*, 2008). Although it is technically acceptable to use

“CYP3A” to indicate the expression or activity of any of the four isoforms, it must be noted that CYP3A4 and CYP3A5 are the two most predominant isoforms in adult humans.

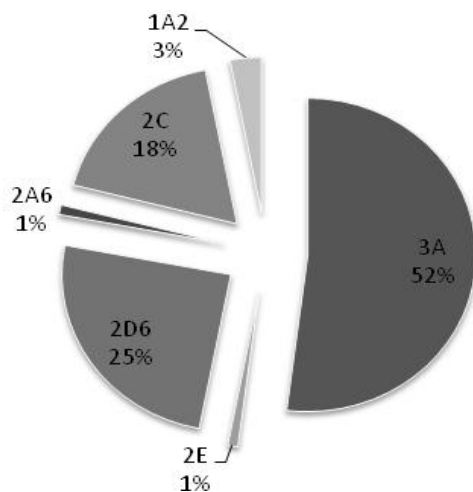


Figure 6 Contribution of CYP450 in drug metabolism.

<https://www.oatext.com/Genetic-polymorphisms-of-drug-eliminating-enzymes-and-transporters>.

Table 3 General characteristics of CYP1-3 in human

Enzyme	Marker-substrate reaction	Substrate specificity	Main tissue localization
CYP1A1	EthoxyresorufinO-deethylation	Pre-carcinogens	Extrahepatic
CYP1A2	PhenacetinO-deethylation.	Aromatic, amines	Liver

	ethoxyresorufinO- deethylation		
CYP1B1	Estradiol-4- hydroxylation	oestradiol	Extrahepatic
CYP2A6	Coumarin hydroxylation	7- Nicotine	Liver
CYP2A13	Coumarin hydroxylation	7-	Olfactory mucosa
CYP2C8	Taxol hydroxylation		Liver
CYP2C9	Tolbutamide methylhydroxylation,	Drugs	Liver

	losartan		
	hydroxylation,	S-	
	warfarin	7-	
	hydroxylation		
CYP2C19	S-mephenytoin4- hydroxylation, omeprazole5- hydroxylation	Drugs	Liver
CYP2D6	DextromethorphanO- deethylation, bufuralol 1'- hydroxylation, debrisoquine4- hydroxylation	Drugs	Liver
CYP2E1	Chlorzoxazone6- hydroxylation	drugs, carcinogens	pre- Liver

CYP2F1	Not known	Not known	Lung
CYP2J2	Arachidonic acid hydroxylation	Fatty acids	Extrahepatic
CYP2R1	Vitamin D hydroxylase	Vitamin D	Extrahepatic
CYP2S1	Trans-retinol oxidation	Small aromatic hydrocarbons	Extrahepatic
CYP3A4	Testosterone 6 β -hydroxylation, midazolam 1'-hydroxylation,	Drugs	Liver, intestine

	erythromycin <i>N</i> - demethylase			
CYP3A5	Testosterone6b- hydroxylation, midazolam 1'- hydroxylation, erythromycin <i>N</i> - demethylase	Drugs		Liver, intestine
CYP3A7	Testosterone 6b- hydroxylation, midazolam 1'- hydroxylation, erythromycin <i>N</i> - demethylase	Drugs		Liver, intestine
CYP3A43	Not known	Not known		Not known

1.1.7 CYP3A enzyme in the brain

It is well established that cytochrome P450 (CYP) 3A enzymes play an important role in drug metabolism in humans. Their function in the liver and intestinal tissues has been extensively studied. However, their expression and functional activity in the brain are not clearly understood. Studies conducted on both humans and rodents have shown that both species contain several different CYP enzymes, including CYP3A, in the brain (Woodland *et al.*, 2008; Kuban and Daniel, 2021). These enzymes also metabolize a number of psychoactive drugs and may significantly impact the efficacy and safety of the drugs. Even though the CYP isoforms in the liver and the brain are almost alike, there may be functional changes between the two (Miksys and Tyndale, 2002). Local brain metabolism of drugs at their site of action may affect therapeutic efficacy differently from liver metabolism, and this difference leads to diversity in the brain-drug response. Moreover, the CYPs subcellular localization of the brain differs from the hepatic CYPs due to variation in cellular structures of hepatocytes and neurons. Immunoblotting and immunohistochemistry research findings on whole brains of rats show that the expression of total CYP enzymes in the brain is only about 10% of that in the liver (Warner *et al.*, 1988; Gervasini *et al.*, 2004). The studies indicated that CYP3A is found in the cerebellum, olfactory bulbs, hypothalamus, and striatum of the rat brain. It was found that the total mRNA level of *Cyp3a1* in the rat brain was only 0.02% of that in the rat liver (Schilter and Omiecinski, 1993). Notwithstanding these low levels, various drugs used to treat central nervous system (CNS) conditions are CYP3A substrates, and their action in specific areas of the brain may cause therapeutic failure or drug-induced toxicity. Furthermore, studies have found CYP3A enzyme isoforms in the mitochondrial and microsomal fractions of several brain parts in both rats and humans. It was found that microsomes from rats contained small amounts of 6-hydroxy

testosterone after testosterone incubation (Jayyosi *et al.*, 1992). It is hypothesized that the enzyme CYP3A is responsible for the conversion of testosterone to its 6-hydroxylated metabolite. The author also discovered a significant immunoreactive band in the brain mitochondria and a minor band in the brain microsomes. Compared to the microsomes, the considerably predominant band in the mitochondria was linked with 40% lower 6-hydroxy testosterone formation in the mitochondria. Moreover, the anti-cytochrome P450p antibody did not impact the 6-hydroxy testosterone production. Therefore, the research could not ascertain CYP3A activity in the rat brain, and the effect of cytochrome P450p-related immunoreactive protein in rat brain mitochondria must be studied further.

Using Western blot analysis, Rosenbrock *et al.* (1999) showed that CYP3A was present in substantially lower amounts in the brain microsomes than in the liver microsomes. They were also able to detect relatively low amounts of 6 β -hydroxy testosterone after long incubation times of 2–6 h. The production of 6 β -hydroxy testosterone was induced by five times after a 3-week oral treatment with phenytoin. However, inhibitory experiments with the anti-CYP3A antibody lowered the formation of 6 β -hydroxy testosterone only marginally (8%), whereas the anti-CYP2B1/2 antibody decreased the formation of the metabolite at a much higher level (35%). Based on these experiments, it can be suggested that 6 β -hydroxylation of testosterone in the rat brain is not a suitable analysis for determining CYP3A activity in the rat brain. Certain immunoblotting investigations indicate that the presence of Cyp3a1/2 protein is substantially more in the brain mitochondrial fraction than in the microsomal fraction contrary to what is observed in the liver (Jayyosi *et al.*, 1992).

A Northern blotting experiment revealed that Cyp3a9 is transcriptionally expressed in the rat brain (Wang *et al.*, 1996). The inducibility of Cyp3a9 was by using dexamethasone. However, the blotting analysis revealed no substantial increase of CYP3A9 mRNA in rat brain when dexamethasone was used. This finding supported Jayyosi *et al.* observation that testosterone metabolism by rat brain microsomes was not inducible. Furthermore, fluorescence in situ hybridization was performed to show the existence of Cyp3a mRNA in neuronal cells of the rat cortex, cerebellum, hippocampus, and thalamus (Pai *et al.*, 2002). Recently, the expression of Cyp3a1 mRNA, but not Cyp3a2 mRNA, was confirmed in male rat brain micro-vessels by RT-PCR (Mei *et al.*, 2004). All these findings supported the presence of CYP3A in microsome and mitochondria in the rat brain.

1.1.8 CYP3A activity in the brain

Low levels of CYP expression in the brain prove that the brain plays a minimal role in drug clearance. However, for medications that can cross the blood-brain barrier, including the functional barrier created by efflux pumps, CYP-mediated biotransformation may be crucial for their efficacy, or lack of it (Britto and Wedlund, 1992). Hence, it is essential to understand CYP activity in different compartments of the brain to optimize medication for many CNS disorders. In addition, many endogenous and exogenous CYP3A substrates have been shown to be metabolized by brain fractions prepared from different species including mice, rats, monkeys, and humans (Martignoni *et al.*, 2006). For instance, the demethylation of amitriptyline to nortriptyline in rat and human brain microsomes has been shown to be CYP3A-mediated, as seen in its suppression by ketoconazole and a monoclonal antibody specific for CYP3A4 (Voirol *et al.*, 2000). In an initial study published in the same article, it was shown that CYP3A4 was the main isozyme to participate in the metabolism of Midazolam, with only a minimal production of 1-hydroxymidazolam,

possibly due to reduced sensitivity of the assay. Several studies have shown qualitative variations in the metabolism of CYP3A between the liver and the brain. For example, the production rate of two CYP3A metabolites of alprazolam were shown to be different in microsomes taken from entire brains of rats than in liver microsomes (Pai et al., 2002). As hypothesized, rat liver microsomes metabolized alprazolam at a much higher rate (30-fold) than rat brain microsomes, but the difference in the rate of production of the minor metabolite, 1-hydroxyalprazolam (1-OHA), was much smaller (1.3-fold higher in liver than in brain). It may be therapeutically significant that the brain generates more 1-OHA than 4-OHA compared to the liver, as 1-OHA is more pharmacologically active (77% of a parent) than 4-OHA (14% of a parent). Recent research has explored the catalytic activity of rat Cyp3a1 in the brain using erythromycin as a substrate (Yadav *et al.*, 2006). Brain microsomes obtained from Wistar rats had 11-fold lower erythromycin demethylase activity than liver microsomes. Erythromycin demethylase activity increased 3- to 4-fold in the liver and 1.5- to 2-fold in the brain following dexamethasone and pregnenolone-16-carbonitrile (PCN) pretreatment of rats, but it remained constant following phenobarbital pretreatment.

- **Use of midazolam as a probe agent for CYP3A phenotyping**

Midazolam is a benzodiazepine sedative-hypnotic with a short half-life that the FDA has approved for use in inducing anesthesia and sedation. Midazolam is metabolized to two primary hydroxylated metabolites, 1'hydroxymidazolam (1'OH-MDZ) and 4'hydroxymidazolam (4'OH-MDZ) by CYP3A4 and CYP3A5 Figure 7 (Jabor *et al.*, 2005). Midazolam has frequently been used as a probe drug to assess CYP3A function in healthy subjects due to its nearly complete

metabolism by CYP3A and lack of affinity for transporters, as well as its short half-life and favorable safety profile (Chaobal and Kharasch, 2005).

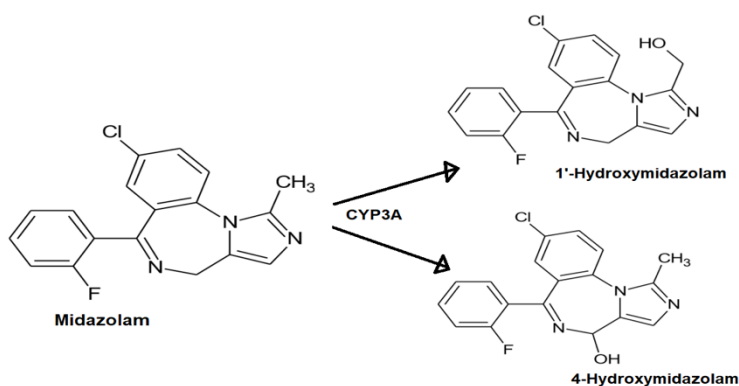


Figure 7 Chemical structure of midazolam and its major metabolite.

1.1.9 Implications of P450 on brain cell

The blood-brain barrier (BBB) and the blood-cerebrospinal fluid (CSF) barrier are important factors for managing the composition of the cerebral environment. The formation of central nervous system (CNS) barriers prevents many drugs and xenobiotics from entering the brain due to structural changes, such as the development of tight junctions, which are responsible for this restriction (Abbott, 2005). The entry of the drug into the brain is controlled by efflux transporters that are ATP-dependent and membrane-bound, as has been shown in several studies of the BBB and blood-CSF barrier cells. It has been demonstrated that lipophilic compounds used in CNS therapy are substrates for drug efflux transporters expressed on the luminal side of the cerebrovascular system (Marchi *et al.*, 2004). This is one of the processes causing medication resistance in ailments of the central nervous system. Recent research has found that the P450 enzymes in the brain are also critical in the treatment of psychosomatic disorders. CYP enzymes

are heme-containing proteins that, along with their involvement in drug metabolism in the liver, are functionally active in the neurovascular unit and are expressed in other brain cells (Ghosh *et al.*, 2011).

In contrast to drug transporters, the biotransformation of a parent drug into a metabolite can have major pharmacological consequences, altering the affinity and final efficacy of a drug on a given target. The discovery of xenobiotic-metabolizing enzymes in humans has led to the speculation whether this class of enzymes is involved in the development of illness or not (Dutheil *et al.*, 2008). Pharmacological reactions in the brain are influenced by drug biotransformation, which may affect local pharmacological reactions and cause adverse effects. Although CYP levels in the brain are typically lower than those in the liver, it has been suggested that changes in CYP brain biotransformation play a role in the failure or toxicity of central nervous system (CNS) medications. Brain P450 expression may become even more pronounced in the presence of CNS ailments and cancer.

Epilepsy: Many factors affect antiepileptic medication (AED) efficacy, including drug metabolism and delivery to the target sensitivity. Recently, it was proposed that neurovascular P450s have a role in the epileptic brain (Ghosh *et al.*, 2011). Therapeutic efficacy or the development of neurotoxic metabolites may be lost due to the local metabolization of AEDs. In human hippocampus pyramidal neurons, AEDs such as oxcarbazepine, carbamazepine, and phenytoin are associated with CYP3A4 (Killer *et al.*, 2009). Thus, inducing CYP3A4 metabolism in the brain can potentially change brain function. The localization of CYP3A4 in the microvessels and neurons of a drug-resistant epileptic brain has been demonstrated by using an immunohistochemistry study. Non-neurological autopsy brain tissues have unexpectedly shown lower levels of CYP3A4 than drug-resistant epileptic brains. Moreover, previous studies have

found that CYP3A4 mRNA expression was substantially higher in epileptic brain endothelial cells isolated from the drug-resistant epileptic brain (Ghosh *et al.*, 2010; Ghosh *et al.*, 2011). Compared to patients with untreated epilepsy, patients treated with AED have higher expression of CYP3A4 in the hippocampus area (Killer *et al.*, 2009).

Cancer: P450 enzymes' existence in tumor cells has been linked to tumor formation, the reason being that specific P450 enzymes perform essential cellular functions such as inactivating antitumor drugs or activating tumor-promoting drugs (McFadyen *et al.*, 2004). This emphasizes the key role of CYPs in balancing cytotoxicity and protection. Research has shown that the concentrations of ellipticine required to kill a glioblastoma cell line are dependent on CYP1A1, CYP1B1, and CYP3A4-mediated biotransformation, confirming a link between P450s and anticancer activity (Martinkova *et al.*, 2009).

1.1.10 Interindividual Variability in Cytochrome P450

It has been established that 15–20% of the drug candidate is affected by the polymorphism of CYP genes (Sikka *et al.*, 2005). Polymorphism of CYPs enzymes is a variation related to changes in the amino acid sequence of the coding region and is responsible for some of the basal interindividual variation in P450-mediated metabolism in humans. In the presence of genetic polymorphism, individuals within a certain group of people are separated into a minimum of two phenotypes, poor metabolizers (PMs) and extensive metabolizers (EMs), based on their abilities to metabolize a particular probe drug. When the parent molecule is processed exclusively by the polymorphic enzyme, poor metabolizers have the insufficient metabolizing ability, generally, create higher drug concentrations, and may exhibit adverse effects or toxicity. In comparison, EMs may exhibit subtherapeutic levels at standard doses or may require greater doses to get a

therapeutic response. If the synthesis of an active metabolite is required for therapeutic action, PMs may fail, while EMs may have a higher risk of side consequences (Fukasawa *et al.*, 2007).

AIMS OF THE STUDY

The main purpose of this study is to compare the content and metabolic activity of CYP3A in the brain microsomal and mitochondrial fractions. To achieve this goal, we developed a CYP3A functional assay in rat brain mitochondria and microsomes to determine the Michaelis-Menten kinetics of the formation of CYP3A-mediated hydroxylated metabolites of midazolam, as a substrate of CYP3A, by UPLC-MS/MS. Additionally, we analyzed the protein levels of CYP3A in the rat brain mitochondria and microsomes by western blot analysis.

Hypothesis

Brain microsomes and mitochondria contribute differently to the local (brain) metabolism of centrally acting CYP3A substrates.

Specific aims

- To establish the Michaelis-Menten kinetics of CYP3A activity in the rat brain microsomes and mitochondria using midazolam as a substrate probe.
- To determine the relative abundance of CYP3A protein in the rat brain microsomes and mitochondria by Western blot analysis.

CHAPTER 2

2.1 Chemicals and antibodies

Midazolam (MDZ) (1443602) was purchased from Sigma Aldrich. Analytical metabolite standard solutions for 1'-hydroxymidazolam (H-922) was purchased from Cerilliant and 4-hydroxymidazolam (UC431) was purchased from Sigma Aldrich. Stable isotope of 1'-hydroxymidazolam d5 (KIT1925) and 4-hydroxymidazolam d5 (H948427) were purchased from Toronto research chemicals. The primary antibodies, polyclonal CYP3A2 (ab195627), Calreticulin (Ab92516), and VDAC1 (Ab15895), which are raised in rabbit, were purchased from Abcam (Cambridge, MA, USA). The secondary antibody, Goat Anti-Rabbit IgG H&L (Ab6721), was purchased from Abcam. The other reagents and compounds were obtained from commercial sources.

2.2 Experimental

2.2.1 Animals

Animal studies were approved by the Chapman University Institutional Animal care and Use Committee. Adult male Sprague-Dawley rats (234-274 g) were purchased from Charles River Laboratories (Wilmington, MA, USA). The rats were housed in a temperature- and humidity-controlled room under a 12 h light-dark cycle with free access to food and water. Rats were anesthetized using isoflurane (induction 3-5% and maintenance 1-3% of isoflurane). After opening the chest, the whole-body perfusion to remove blood was conducted through perfusion of the left ventricle using a 22-gauge needle and cold saline (0.9%, w/v) at a flow rate of 25

mL/min for 8 min., The right atrium was cut to allow the blood to flow out. Then, brains were collected, snap-frozen in liquid nitrogen and stored at -80C.

2.2.2 Preparation of microsomal and mitochondrial subcellular fractions

The differential centrifugation technique is shown schematically in Figure 8 and described below. Frozen whole brains (n = 8) from adult rats were weighed and homogenized in an ice-cold buffer (100 mM Tris, 0.2 mM EDTA, 1.15% KCl, pH = 7.4) at a 1:10 ratio, using 50 mL potter-Elvehjam tubes, applying ten strokes with a motor-driven Teflon pestle. All subsequent steps were performed on ice (4°C). Cell debris and nuclei were removed by centrifugation at 1300 g for 5 minutes (run twice). The supernatants were centrifuged at 21,000 g for 12 minutes to separate the crude mitochondrial (pellet) and the combined cytosolic and microsomal (supernatant) fractions. The supernatant was collected into a 70 ml Polycarbonate tube (PC) ultracentrifuge tube and centrifuged twice at 110,000 g-force for 70 minutes to prepare microsomes. The resulting microsomal pellet was resuspended and homogenized with Potter-Elvehjem homogenizer in 1.5 ml of storage buffer (100 mM Tris, 0.2 mM EDTA, 1.15% KCl, 20% glycerol, 0.1 mM dithiothreitol, 22 µM butylated hydroxytoluene, and 0.1 mM phenylmethylsulfonyl fluoride; pH 7.4) and stored at -80°C. The mitochondrial pellet was resuspended in a 15% Percoll solution to purify the crude mitochondrial fraction. The purification was run on a 15%, 24%, and 40% percoll gradient in 10 mL PC tubes and centrifuged at 30,700 g-force for 12 min. During centrifugation, purified mitochondria initially layered on the density gradient will sediment until they arrive at the region of the gradient where the density of the suspension is equal to their own. Thus, the layer containing pure mitochondria at the interface of the 24% and 40% Percoll layers were collected and washed 3 to 4 times with the homogenizing buffer by centrifugation at 21,000 g-force for 12

minutes. The pellet was resuspended and homogenized with Potter-Elvehjem homogenizer in 0.5 ml of storage buffer and stored at -80°C , until required.

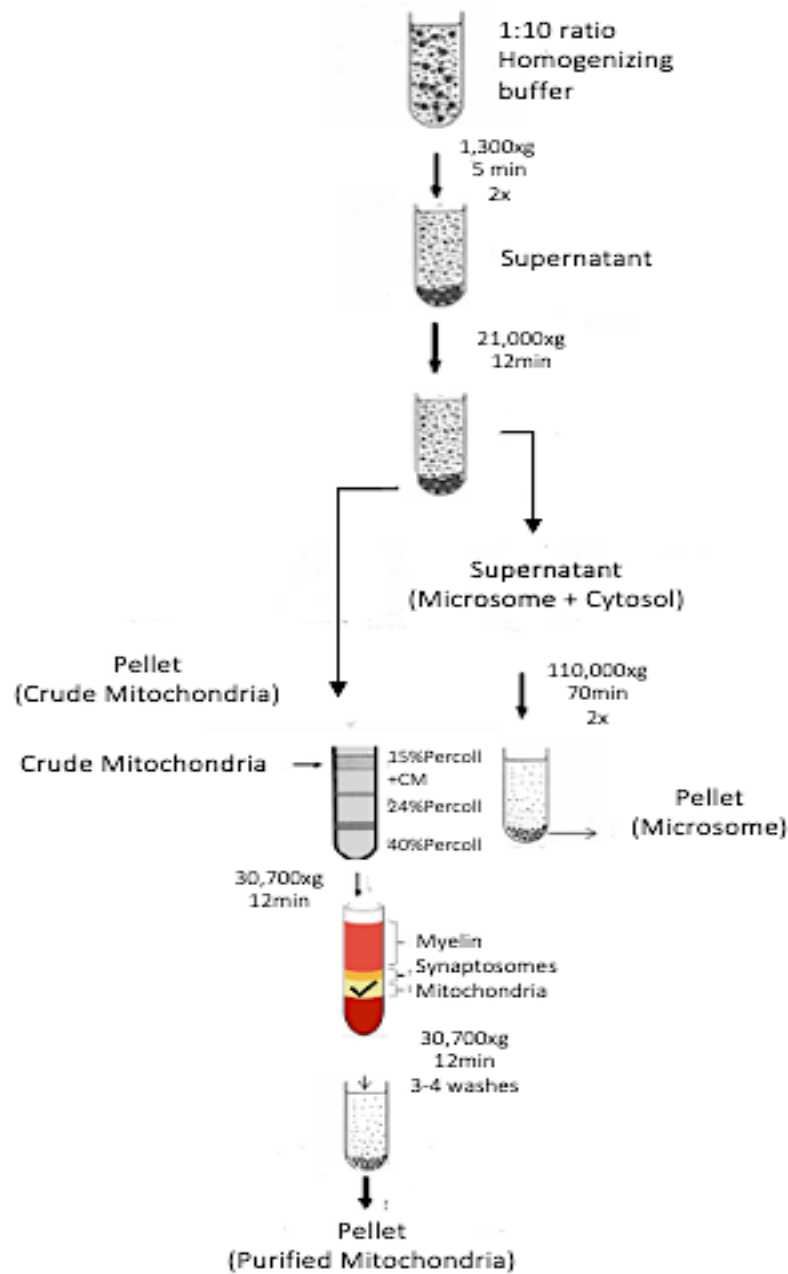


Figure 8 Preparation of Microsome and Mitochondria.

2.2.3 Protein concentration determination

The concentration of protein in brain microsomal and mitochondrial fractions was determined by Bicinchoninic acid (BCA) protein assay. Microsomal and mitochondrial samples were diluted to specific dilutions with 100 mM potassium phosphate buffer (pH 7.4). Bovine serum albumin (0-2 mg/ml) was used to construct the protein standard curve. 25 μ l of standards and samples were assayed in triplicate into 96 wells. 200 μ l of BCA working reagent was added to each well and incubated at 37°C for 30 min. The plate absorbance was measured at 562 nm by the spectrophotometer (BIO-RAD, iMark, Microplate Reader, Hercules, CA).

2.2.4 Validation of the purity of the subcellular fractions

Calreticulin (Rabbit antibody) was used as a marker for the brain microsomal fractions and VDAC (Rabbit antibody) was used as a marker for the brain mitochondrial fractions.

Microsomal and mitochondrial samples from 8 rat brains were diluted to 1 mg/ml with 1xTBS. Loading buffer (100 μ l of 2-b-mercaptoethanol and 900 μ l of 4x Laemmli sample buffer, BIO-RAD, Hercules, CA) was added to each sample at a ratio of 3:1 and heated in 95°C water for 5 minutes. Proteins (10 μ g) were subjected to SDS-polyacrylamide gel electrophoresis on a precast Bio-Rad (Hercules, CA, USA) 4-20% MP TGX Stain-Free gels at constant voltage (200 V) for 30 minutes. Proteins were transferred onto PVDF membranes using the Bio-Rad Trans-Blot Turbo Transfer System; then, the membrane was blocked with 5% BSA for 1 hour at room temperature. Subsequently, the membrane was incubated overnight with the primary antibody in a cold room at 4°C: calreticulin (1:10,000), or V-DAC1 (1:50,000). After washing, membranes

were incubated with the secondary antibody (Abcam, Goat Anti-Rabbit) diluted in wash buffer with StepTactin-HRP ladder solution (1:50,000) for 1 hour at room temperature on a shaker. Then, bands are visualized with the Bio-Rad ChemiDoc Imager system. The intensities of VDAC1 bands in mitochondria and calreticulin bands in microsomes were considered as 100%, and the percent impurities of VDAC1 in microsomes (mitochondrial contamination) and calreticulin in mitochondria (microsomal contamination) were subsequently estimated.

2.2.5 Determination of midazolam hydroxylase activity

Base-powder of commercial Midazolam was dissolved in 105 mM HCl to give a stock solution of 5000 μ M (50 mM). The primary stock solutions of Midazolam (50 mM) were further diluted with 5 mM HCl to make working solutions of 50, 100, 250, 500, 1000, 2500, 5000, and 10000 μ M for assessing microsome CYP3A enzymatic assay and 250, 500, 1000, 2500, 5000, 10000, 15000, 25000, and 50000 μ M for assessing mitochondria CYP3A enzymatic assay. Two independent runs side-by-side were performed to ascertain the differences between microsome and mitochondria activities, one set for microsome and the other set for mitochondria. The reaction mixture (25 μ L) in 100 mM Tris-HCl buffer, pH 7.4 (15 μ L) contained 0.25 mg/ml rat brain microsomes or mitochondria (2.5 μ L of a 2.5 mg/ml microsomal or mitochondrial suspension), 20 mM Mg Cl₂ (2.5 μ L of 200 mM stock) and 1 mM NADPH (2.5 μ L of 10 mM stock). The mixtures were vortexed and pre-incubated for 5 minutes, maintained at 37°C. The reaction was initiated by adding the 2.5 μ L of MDZ stock solutions to get the final conc. ranging from 5 to 1000 μ M for microsome and 25 to 5000 μ M for mitochondria with an incubation time of 10 minutes. The reaction was stopped by the addition of 75 μ l acetonitrile, containing 10 nM 1'-OH-d5 and 4-OH-d5 as internal standards. The reaction mixtures were vortexed, placed on ice for 5 minutes, centrifuged for 5

minutes at 13,400 rpm, and injected onto the LC-MS/MS system. The incubation time of 10 min and the protein concentration of 0.25 mg/mL were based on previous studies, investigating the time and protein linearity in microsomes (Devaraj et al., 2021).

2.2.6 Liquid chromatography–mass spectrometry (LC-MS/MS)

2.2.6.1. Instrumentation

The mass spectrometric data for midazolam, metabolites (1'-hydroxymidazolam & 4-hydroxymidazolam), and their respective deuterated internal standards (1'-hydroxymidazolam-d5 and 4-hydroxymidazolam-d5) were generated using Bruker EVOQ triple quadrupole mass spectrometer, as described before (Devaraj et al, 2021). Chromatography was performed on a Kinetex 1.7 μ m C18 (100 \times 2.1 mm, 100 Å) column (Phenomenex Inc; Torrance, CA, USA), preceded by a Phenomenex C18 Security Guard ULTRA (2.1 mm) pre-column. All chromatographic separations were performed at a flow rate of 0.250 mL/min under gradient conditions described in Table 4. Mobile phase A consisted of 5 mM ammonium formate in LCMS water, and mobile phase B consisted of 100% acetonitrile. All other LC-MS/MS setting for CYP3A assay are shown in (table 4).

Table 4 LC/MS/MS setting for CYP3A

Column	: Kinetex, C18, 1.7 μ m, 100 mm x 2.1 mm
Mobile phase A (aqueous)	5mM ammonium formate in LCMS water

Mobile phase B (Organic)	100% Acetonitrile		
Column Temperature	40°C		
Flow rate	0.25 mL/min		
Gradient conditions (min)	Time (min)	Mobile phase A (%)	Mobile phase B (%)
	0.00	70	30
	1.20	70	30
	5.00	30	70
	6.00	30	70
	6.00	70	30
	7.50	70	30
MRM transitions and Retention time	1'-hydroxymidazolam 342 -> 202.9 (quantifier ion) Retention time = 4.69 minutes		

	<p>d₅-1'-hydroxymidazolam 346.9 -> 207.9 (quantifier ion)</p> <p>Retention time = 4.69 minutes</p> <p>4-hydroxymidazolam 342 -> 233.9 (quantifier ion)</p> <p>Retention time = 4.4 minutes</p> <p>d₅-4-hydroxymidazolam 346.9 -> 234.9 (quantifier ion)</p> <p>Retention time = 4.4 minutes</p> <p>Midazolam 326 -> 290.9 (quantifier ion)</p> <p>Retention time = 5.5 minutes</p>
<p>Source Conditions:</p>	<p>Source type = Heated Electrospray Ionization (HESI-II)</p> <p>Spray Voltage = 3000V (positive mode)</p> <p>Cone temperature = 300⁰C</p> <p>Cone gas flow = 25psi</p> <p>Heated probe temperature = 400⁰C</p> <p>Heated probe gas flow = 40psi</p> <p>Nebulizer gas flow = 50psi</p>

2.2.7 Stock solution preparation

The primary stock solution of 1'-hydroxy midazolam (metabolite) comes as a 1 mg/mL in methanol from Cerilliant. This stock's concentration is 2926 μ M, while 4-hydroxy midazolam solution (metabolite) comes as a solid powder from Sigma. Stock solution of 1 mg/mL is prepared in methanol and this stock's concentration is 2926 μ M. For the internal standards, the stock solution of 1'-hydroxy midazolam-d₅ solution comes as a 100 μ g/mL in methanol from Toronto research chemicals, stock's concentration is 289 μ M. For 4-hydroxy midazolam-d₅ solution, it comes as a powder from Toronto research chemicals. Stock solution of 2 mg/mL is prepared in DMSO, and this stock's concentration is 5780 μ M. The primary stock solutions of 1'-OH-MDZ and 4-OH-MDZ were further diluted with 100 mM Tris-HCl buffer (pH 7.4) to make working solutions of 10, 20, 50, 100, 250, 500, 750, and 1000 nM for the preparation of calibration curves and 10, 30, 300, and 800 nM for quality control (QC) samples. The primary stock solutions of the internal standards were further diluted in acetonitrile to prepare a 10 nM solution.

2.2.8 Preparation of Calibration standards and quality control samples

Calibration standards and quality control samples were prepared in a in the rat brain microsomes and mitochondria at metabolite concentration range between 1 nM to 100 nM in a final volume of 25 μ L. The calibration standards contained 0.25 mg/mL brain microsomes or mitochondria and 20 mM MgCl₂ in 100 mM Tris buffer pH 7.4. The working solutions of the two metabolites were added to the matrix to make final concentrations of 0 (blank), 1, 2, 5, 10, 25, 50, 75, and 100 nM for calibration curve standard, and 3, 30, and 80 nM for the preparation of quality control samples. Then, 75 μ L of 10 nM of both 1-OH-MDZ-d₅ and 4-OH-MDZ-d₅ as internal

standards were added to each calibration standard and quality control sample tubes. After vortex-mixing, the samples were centrifuged at 13,400 rpm for 5 min. Aliquot (90 μ L) of the samples were transferred into HPLC vials and 5 μ L of the sample was injected onto LC-MS/MS.

Calibration curves for each of the two MDZ metabolites were constructed by plotting the peak area ratios of each analyte: internal standard against the concentrations of the metabolite in the samples using a weighting factor of $1/x$, where x is the added concentration.

2.2.9 Method validation

A partial validation according to the FDA guidelines were performed for quantifying midazolam metabolites (1'-hydroxymidazolam and 4-hydroxymidazolam) in rat brain MC and MT. The analytical method was validated with respect to accuracy and precision. Three independent runs, each consisting of a set of calibration standards and three quality control (QC) levels with five replicates per QC level, were used to verify the assay's precision and accuracy. The QC samples were prepared similarly to the calibrators and tested at the calibration curve's lower (LQC, 3 nM), medium (MQC, 30 nM), and higher (HQC, 80 nM) concentrations of both metabolites. On the same day, five replicates of each QC sample were analyzed against the calibration standards to determine within-run precision and accuracy. Preparing and evaluating calibration standards and QC samples in five replicates on three different occasions was used to assess between-run precision and accuracy. The precision was measured as a percentage of the QC replicates' relative standard deviation (% R.S.D.). The percent relative error (% R.E.) of the measured concentrations versus the theoretical concentrations was used to compute the accuracy.

2.2.10 Western blot analysis of rat brain CYP3A in microsomes and mitochondria

SDS polyacrylamide gel electrophoresis (SDS-PAGE) was carried out using 4-15% MP TGX Stain-Free gels with ten well combs (Bio-Rad, 4568096). Microsomal or mitochondrial samples were diluted to 1 mg/ml concentration with 1x Tris-buffered saline. Laemmli buffer was then added to each sample at a ratio of 3:1 (sample: buffer). The samples were denatured by heating at 95°C for 5 min. After cooling, the samples were applied to wells of the gel with a protein concentration of 40 µg. The gel was then electrophoresed at 120 V for 30-90 minutes until the bromophenol blue had reached the end of the separating gel. Once the gel had finished running, proteins were transferred onto PVDF membranes using the Bio-Rad Trans-Blot Turbo Transfer System with constructing a gel sandwich. When the transfer was complete, the membrane was blocked with 5% nonfat milk prepared in wash buffer (TBS) for 1 hr at room temperature. Then, the membrane was incubated overnight with the primary antibody against CYP3A (1:2500) in a 4°C cold room on an orbital shaker. We used polyclonal CYP3A2 antibody, which is raised in rabbit (ab-195627, Abcam). After incubation with the primary antibody, the membrane was washed and incubated with secondary antibody (1:5000) diluted in wash buffer with StepTactin-HRP ladder for 1 hour at room temperature on a shaker. Bands were visualized with the Bio-Rad ChemiDoc Imager system.

2.3 Statistical Analysis:

The metabolism rate-substrate concentration profiles for microsomal and mitochondrial fractions were analyzed using a single-enzyme, Michaelis-Menten kinetics model, including MM parameters

of maximum velocity (V_{max}) and MM constant (K_m). The nonlinear regression analysis was carried out in GraphPad Prism software (La Jolla, CA, USA) using the pooled data from the eight brains, which generated V_{max} and K_m values and their variability (SE) for each metabolite (1'-OH-MDZ and 4-OH-MDZ) and fraction (microsomes and mitochondria). The differences between the microsomes and mitochondria in their MM kinetic parameters were tested using a two-tailed, t-test analysis. A *p-value* of < 0.05 was considered significant. All the other data analyses were performed using Graphpad Prism. Data are presented as mean \pm SD.

CHAPTER 3

3.1 Result

3.1.1 Preparation and Characterization of Microsomes and Mitochondria

3.1.1.1 Protein yields

Based on obtained results from Bicinchoninic Acid (BCA) protein assay, the average (\pm SD) protein yields were 7.07 ± 1.19 and 1.88 ± 0.53 mg per g brain tissue for microsomes and mitochondria, respectively.

3.1.1.2 Marker proteins Calreticulin and Voltage- Dependent Anion Channel 1 (VDAC1)

Western blot analysis using calreticulin antibody as a microsomal protein marker was used to determine the purity of mitochondria, which corresponds to the MW (48kDa). The results indicated that $19.3 \pm 7.8\%$ of mitochondrial samples were contaminated with microsomes.

VDAC1, a mitochondrial marker with a MW of 31kDa, was used to determine the purity of microsomal samples. According to this finding, microsomal fractions contained $5.93 \pm 3.01\%$ mitochondrial impurity.

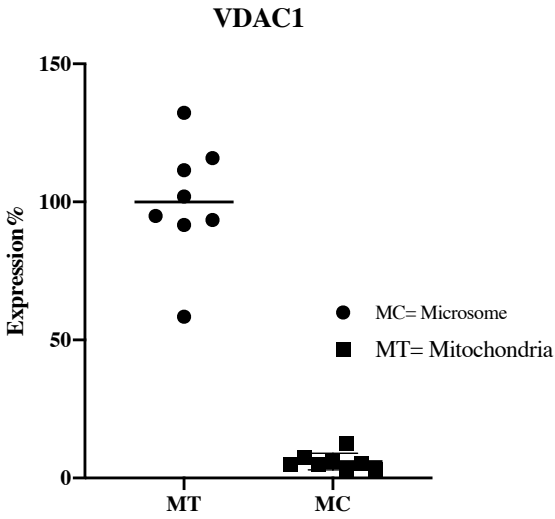


Figure 9 Immunoblot analysis of VDAC1, as a mitochondrial marker. Statistical analysis is based on paired t test. ****P <0.0001

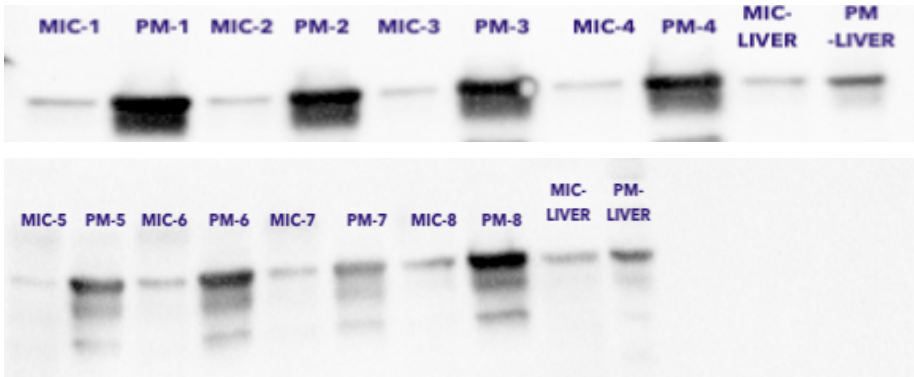


Figure 10 Western blot analysis of VDAC in eight rat brains (MIC=microsome, PM= mitochondria)

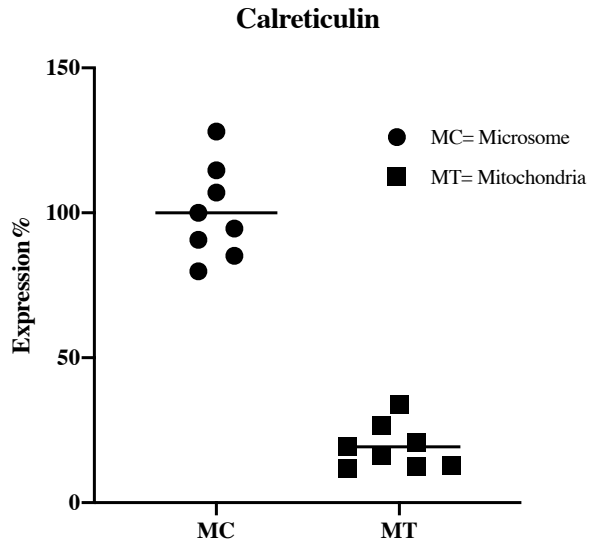


Figure 11 Immunoblot analysis of calreticulin as a microsomal marker. Statistical analysis is based on paired t test. ****P <0.0001.

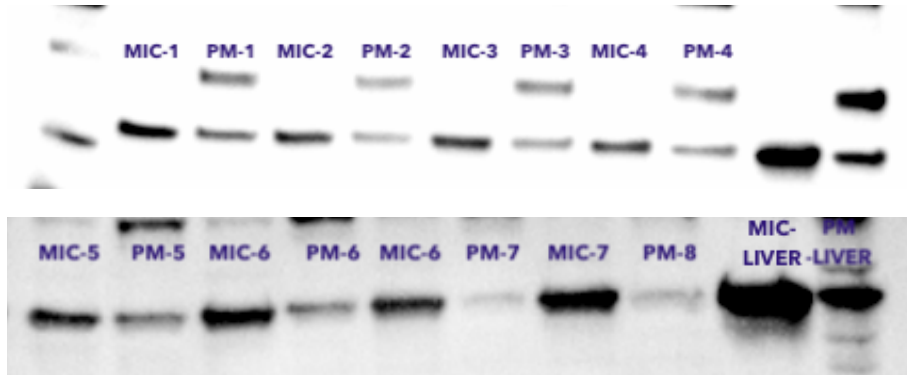


Figure 12 Western blot analysis of calreticulin in eight rat brains (MIC=microsome, PM= mitochondria).

3.1.1.3 Western Blot Analysis of CYP3A2

For CYP3A2, an immunoreactive band corresponding to the MW of ~55 kDa was detected in brain microsomes and mitochondria. Mitochondria exhibited the greatest protein-corrected band intensity ($P < 0.0001$); band intensities are expressed as a percentage of the intensity. Because mitochondria had the highest band intensity, the band intensities of CYP3A2 are presented as a percentage of intensity in the brain fraction of mitochondria. The band intensities of CYP3A2 in the mitochondria fraction ($100 \pm 9\%$) were twice as much as that in the microsomes ($49.2 \pm 13.3\%$) (Fig. 13).

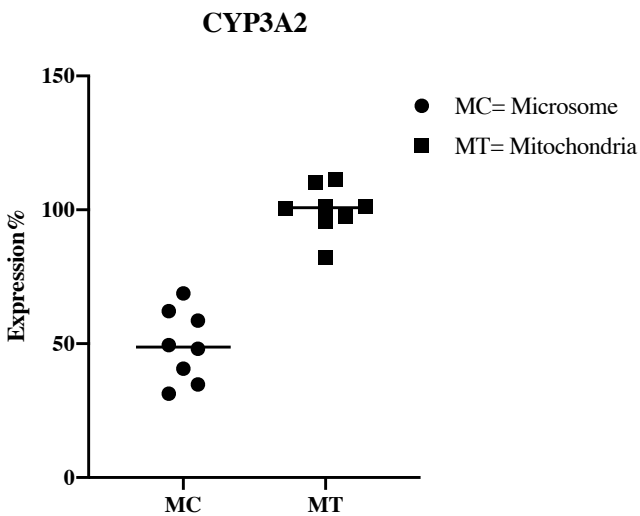


Figure 13 Western Blot Analysis of CYP3A2 in eight independent brain samples.

Statistical analysis is based on paired t test. ****P < 0.0001

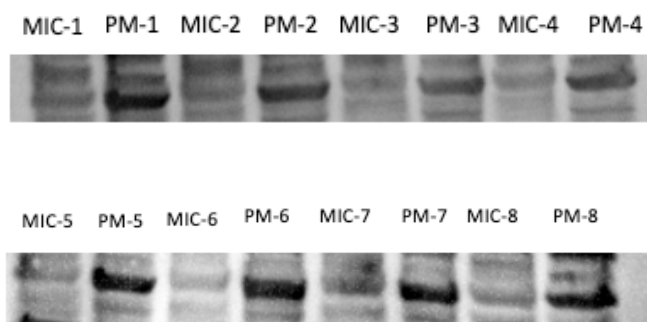


Figure 14 Western blot analysis in eight rat brains (MIC=microsome, PM= mitochondria).

3.1.2 LC-MS/MS analysis

3.1.2.1 Calibration Curve- linearity

To graph the calibration curve of the drug, each of the two MDZ metabolites were constructed by plotting the peak area ratios of each analyte/internal standard against the concentration of the metabolites. As shows in Fig. 15, the calibration curves for both microsome and mitochondria were evaluated to determine the linearity. As a result, curves are linear and reproducible over standard concentration range 1-100nM for 1' and 4 OH MDZ.

A comparison of the calibration curves for microsomes and mitochondria has been performed side by side. As a result, the slope and r^2 values of the microsome and mitochondria calibration curves are very similar. Therefore, we used only microsome calibration curves to determine CYP3A Michalis-Menten kinetics in both brain MC and MT samples. Representative coefficient of r^2 values and slope calculated in microsome, and mitochondria, are described in table 5 and 6. Fig. 16 and 17 show the chromatograms of blank (0), highest (100nM) and lowest (1nM) concentrations in the calibration curve.

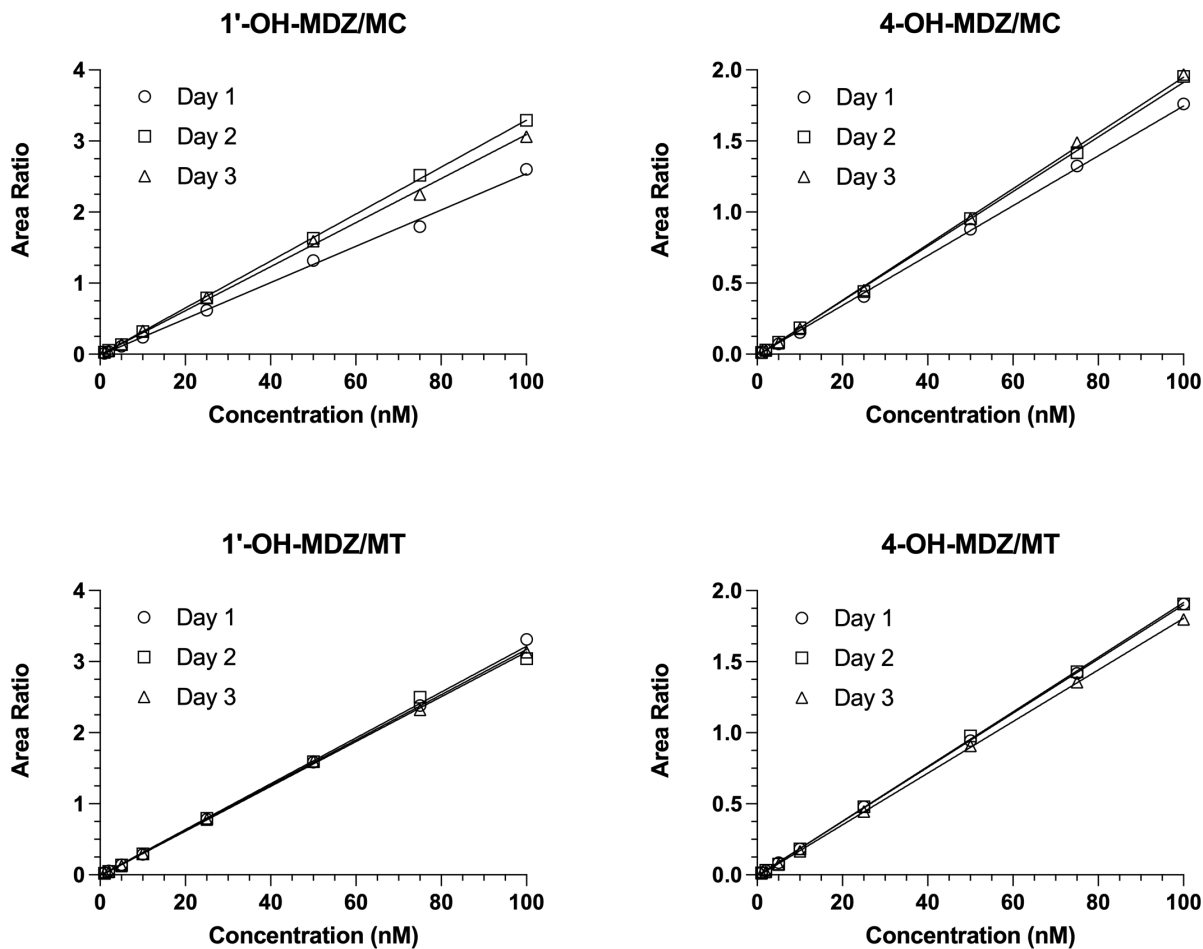


Figure 15 Calibration curve of 1'- and 4- OH MDZ, one set containing rat brain microsomes (0.25mg/mL) and other set containing rat brain mitochondria (0.25mg/mL).

Table 5 4-OH MDZ Slope and coefficient of r^2 in microsomes (MC) and mitochondria (MT).

	Day1		Day2		Day3	
	MT	MC	MT	MC	MT	MC
Slope	0.01905	0.0177	0.01923	0.0194	0.01817	0.0198
R²	0.9998	0.9997	0.9994	0.9994	0.9996	0.9995

Table 6 1'-OH MDZ Slope and coefficient of r^2 in microsomes (MC) and mitochondria (MT).

	Day1		Day2		Day3	
	MT	MC	MT	MC	MT	MC
Slope	0.0322	0.0255	0.0318	0.033	0.0315	0.0309
R²	0.999	0.998	0.998	0.999	0.999	0.999

3.1.2.2 Chromatograms

The spectrometric conditions and other operation parameters were optimized for the detection of Midazolam metabolites in microsome and mitochondria fractions. The peak shapes of the analyte were sharp and devoid of any baseline interferences or overlapping peaks (Fig 16 and 17).

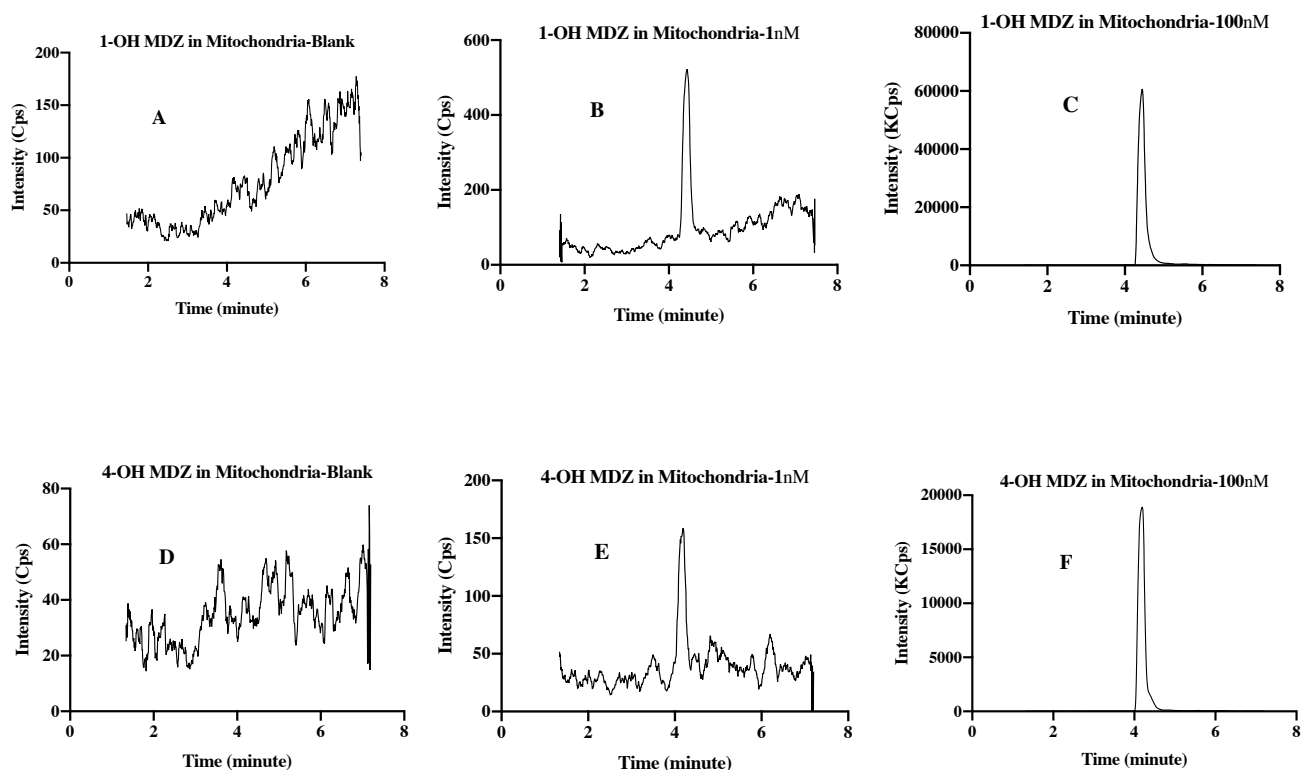


Figure 16 Representative chromatograms of 1-hydroxymidazolam (A, B and C) and 4-hydroxymidazolam (D, E and F) generated from rat brain mitochondria in Blank, 1, or 100 (nM) of 4-hydroxymidazolam and 1-hydroxymidazolam.

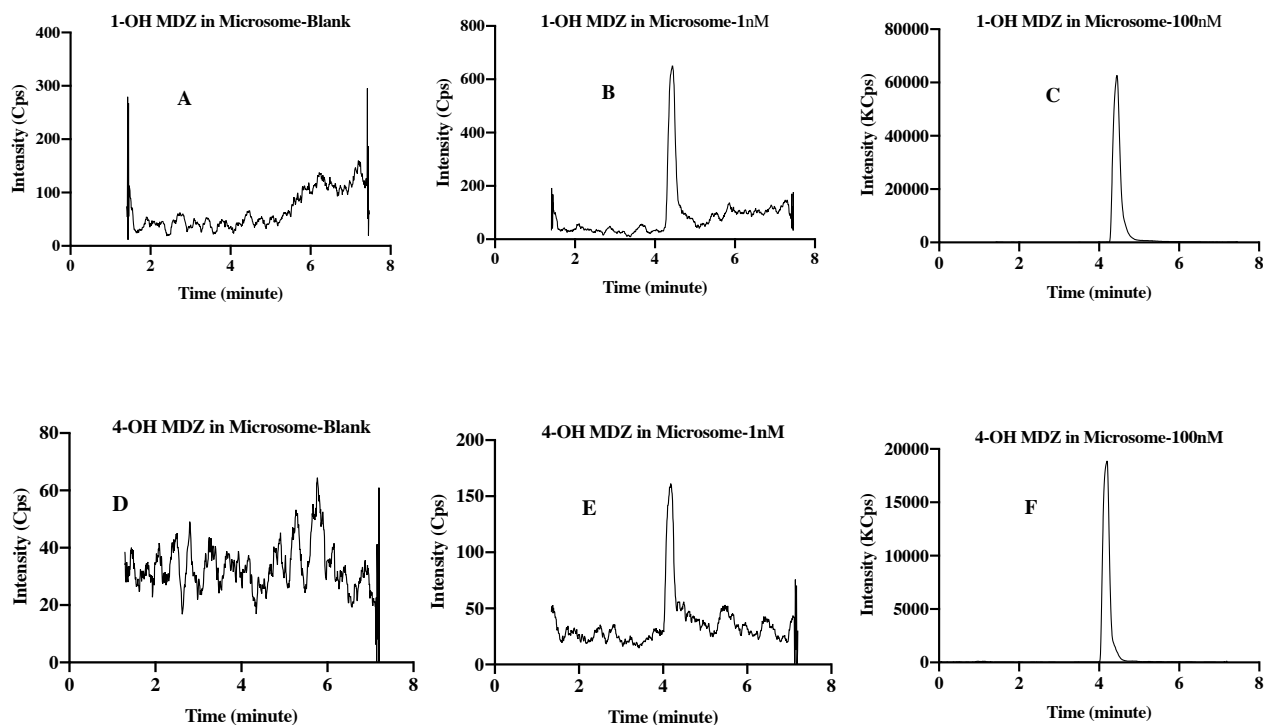


Figure 17 Representative chromatograms of 1-hydroxymidazolam (A, B and C) and 4-hydroxymidazolam (D, E and F) generated from rat brain microsomes in Blank, 1, or 100 (nM) of 4-hydroxymidazolam and 1-hydroxymidazolam.

3.1.2.3 LC-MS/MS method validation-Precision and Accuracy

Partial method validation was assessed as per the US Food and Drug Administration (FDA) bioanalytical method validation guidance. The intra- and inter-run accuracy and precision data for mitochondrial and microsomal samples are presented in Tables 7-10. For mitochondria samples, the intra- and inter-run R.E. values with respect to 4-OH-MDZ ranged from -8.36% to 9.53% and R.S.D. values of $\leq 15\%$. While 1'-OH-MDZ R.E. values ranged from -7.75% to 5.42 and R.S.D. values of $\leq 15\%$. For microsome samples, the R.S.D values in both 1'-OH MDZ and 4-OH MDZ were $\leq 15\%$. The range of R.E. values were between -7.53% to 15.6% for 1'-OH MDZ and -8.52%

to 7.74% for 4-OH MDZ. Precision and accuracy values for both intra- and inter-run experiments were within the acceptable limits in mitochondria and microsome samples.

Table 7 Intra-run precision and accuracy of 4-hydroxymidazolam and 1'-hydroxymidazolam quality control samples in rat brain mitochondria.

Mitochondria 4-OH				
Days	Intra-run (n=5)	Mean	Precision (%R.S.D)	Accuracy (%R.E.)
1	3nM	2.92	6.19	-2.45
2		3.02	6.08	0.617
3		2.74	7.35	-8.36
1	30nM	30.6	6.08	2.15
2		31.0	2.4	3.20
3		32.5	5.83	8.20
1	80nM	84.7	3.37	5.87
2		85.4	3.76	6.83
3		87.6	4.42	9.53
Mitochondria 1-OH				
Days	Intra-run (n=5)	Mean	Precision (%R.S.D)	Accuracy (%R.E.)
1	3nM	2.85	2.23	-4.90

2		3.13	3.21	4.35
3		2.76	3.52	-7.75
1		30.3	3.08	1.13
2	30nM	30.9	3.29	2.91
3		29.6	6.75	-1.37
1		82.8	0.956	3.52
2	80nM	84.3	1.36	5.42
3		79.7	2.46	-0.331

Table 8 Intra-run precision and accuracy of 4-hydroxymidazolam and 1'-hydroxymidazolam quality control samples in rat brain microsome.

Microsome 1-OH				
Days	Intra-run(n=5)	Mean	Precision(%R.S.D)	Accuracy (%R.E.)
1	3nM	3.47	9.03	15.6
2		3.03	5.55	1.04
3		2.77	3.52	-7.53
1	30nM	30.8	6.65	2.68
2		29.8	3.14	-0.522
3		30.5	2.16	1.51
1	80nM	87.1	2.13	8.90
2		76.8	2.17	-3.97
3		84.0	1.32	4.96
Microsome 4-OH				
Days	Intra-run (n=5)	Mean	Precision(%R.S.D)	Accuracy (%R.E.)
1	3nM	3.23	5.89	7.74
2		3.04	4.95	1.20

3		2.74	1.01	-8.52
1	30nM	33.4	10.6	11.4
2		30.7	2.17	2.24
3		29.6	1.95	-1.47
1	80nM	85.1	3.63	6.37
2		79.7	2.86	-0.377
3		83.4	1.76	4.19

Table 9 Inter-run precision and accuracy of 4-hydroxymidazolam and 1'-hydroxymidazolam quality control samples in rat brain mitochondria.

4-OH mitochondria			
Inter-run	Mean	Precision R.S.D	accuracy R.E.
3nM	2.90	7.24	-3.40
30nM	31.4	5.38	4.52
80nM	85.9	3.89	7.41
1-OH mitochondria			
Inter-run	Mean	Precision R.S.D	accuracy R.E.
3nM	2.92	6.18	-2.77
30nM	30.3	4.65	0.900
80nM	82.3	2.87	2.87

Table 10 Inter-run precision and accuracy of 4-hydroxymidazolam and 1'-hydroxymidazolam quality control samples in rat brain microsome.

4-OH Microsome			
Inter-run	Mean	Precision R.S.D	accuracy R.E.
3nM	3.00	8.16	0.14
30nM	31.2	8.22	4.04
80nM	82.7	3.83	3.40
1-OH Microsome			
Inter-run	Mean	Precision R.S.D	accuracy R.E.
3nM	3.09	11.5	3.03
30nM	30.4	4.35	1.22
80nM	82.6	5.68	3.30

3.1.3 CYP3A Michalis-Menten Kinetics

Figure 18 represents the formation rate of 1'-hydroxymidazolam (1'-OH) and 4-hydroxymidazolam (4-OH) in eight independent brain microsome and mitochondria fractions. Fractions were described by the single-enzyme, Michaelis–Menten model. Multiple enzymes were detected in mitochondria. However, due to a lack of sufficient data points to adequately estimate the parameters of a multi-enzyme system, we applied the simpler single-enzyme model to describe mitochondria fraction data. The metabolic rate of 1' and 4-OH MDZ in microsome fractions

plateaued between substrate concentrations of 500 and 1000 μ M. However, the rate of Midazolam metabolites in mitochondria plateaued at 5000 μ M.

Michalis-Menten parameters, maximum velocity (Vmax) and Michaelis-Menten constant (Km) were determined by non-linear regression analysis. Microsomes contained significantly less CYP3A activity. When compared to mitochondria, the 4-hydroxylated metabolite had a 2.5-fold greater maximum velocity (Vmax). In addition, the maximum velocity (Vmax) of the 1'-hydroxylated metabolite was 9-fold greater in mitochondria than in microsomes, and the KM values were 153 times more in mitochondria than in microsomes as well (Table 11 and 12).

Table 11 Maximum velocity (Vmax) and Michaelis-Menten constant (KM) values (mean \pm SD, n = 8 brains) of 1'-OH midazolam metabolites in rat brain microsomes and mitochondria.

1-OH MDZ		
Parameters	Microsome	Mitochondria
Vmax***	0.283 \pm 0.022	2.56 \pm 0.67
Km*	21.7 \pm 15.0	3330 \pm 1640

***, $p < 0.001$; *, $p < 0.047$; Two-tailed, t-test.

Table 12 Maximum velocity (Vmax) and Michaelis-Menten constant (KM) values (mean \pm SD, n = 8 brains) of 4-OH midazolam metabolites in rat brain microsomes and mitochondria.

4-OH MDZ		
Parameters	Microsome	Mitochondria
Vmax*	11.4 \pm 2.0	28.8 \pm 8.2
Km	574 \pm 204	2790 \pm 1540

*, $p < 0.05$; Km, $p > 0.05$; Two-tailed, t-test.

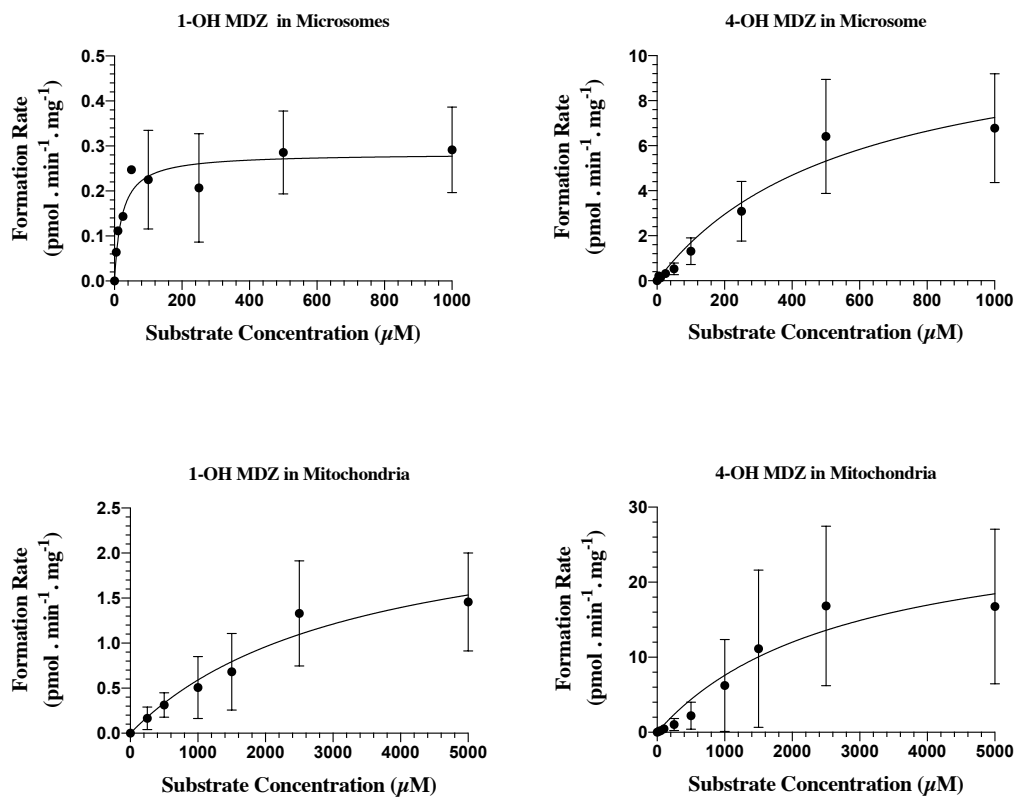


Figure 18 Average rate of 4-hydroxymidazolam and 1'-hydroxymidazolam in mitochondrial and microsomal samples versus different concentrations of midazolam in eight brain preparations.

CHAPTER 4

4.1 Discussion

4.1.1 Content and activity of CYP3A in brain mitochondria and microsome

This study was undertaken to characterize the CYP3A involved in Midazolam metabolism to its metabolites: 1'-hydroxymidazolam and 4-hydroxymidazolam, and thus Michaelis-Menten kinetics of the formation of the metabolites were estimated. Despite the presence of significant quantities of this enzyme in mitochondria (Jayyosi et al., 1992), the enzymatic activity of CYP3A in brain mitochondria has not been identified.

Investigating the kinetics parameters of mitochondria and microsome is important to understand the CYP activity in various brain compartments for optimizing the pharmacotherapy of CNS conditions. Therefore, the study's main goal was to compare the catalytic activity and immunoblotting of CYP3A side by side between the endoplasmic reticulum (microsome) and mitochondria using Midazolam as a substrate probe. The findings suggest that the CYP3A mediated- enzymatic activity as well as immunoblotting in the brain between mitochondria and microsome differed markedly. Generally, correlations were established between the V_{max} and the immunoblotting result. The CYP3A enzyme is less active and has a lower content in microsomes, whereas it is more active and has a higher content in mitochondria. In addition, these results agree that apparent K_m represents the substrate affinity of isoenzyme, whereas apparent V_{max} represents the capacity, which depends on enzyme quantity. Microsomes had a substantially lower V_{max} value than mitochondria. Similarly, the microsome's K_m values were much lower than

mitochondria. There was low apparent K_m (high affinity) and low apparent V_{max} (low capacity) in the metabolic activity of microsomes. In contrast, mitochondria showed high apparent K_m (low affinity) and high apparent V_{max} (high capacity). The revelations in mitochondria would be helpful to design appropriate therapeutic strategies and prevent toxicity.

Possible explanations for the metabolic rate differences between microsomes and mitochondria should be divided into two parts for discussion: differences in the electron transfer system in the subcellular fractions and/or cytochrome P450 isoform activities. The main factor contributing to low affinity in mitochondria might be related to the electron transfer system in eukaryotic cells, including adrenodoxin (Adx), which functions as an electron donor in all mitochondrial cytochrome P450. Wada and Waterman (1992) determined that the adrenodoxin binding site of mitochondrial P450s involved basic amino acid, position 377 and 381 of bovine P450, which are exclusively conserved among all mitochondrial P450s but not among microsomal P450s. According to their results, substituting amino acids at these positions led to dramatic decreases in affinity for adrenodoxin. In addition to their substantial differences in localization, mitochondrial P450s differ from their microsomal counterparts in terms of substrate specificity and structural properties, as well as in respect of their enzymatic activity. Therefore, the differences between microsomes and mitochondria could also be due to the choice of probe and the involvement of more than one isoform of CYP3A. For instance, it has been reported that 3-methylcholanthrene selectively increased the high-affinity component of Phenacetin O-deethylase activity in rat liver microsomes. In contrast, phenobarbital selectively increased the low-affinity component (Kahn *et al.*, 1987). For this reason, it is necessary to clarify CYP isoform-specificity for these activities in the rat brain.

In Western blot analysis, the level of expression of CYP3A2 in mitochondria showed very intense bands compared to microsomes. This is in agreement with the data reported by Jayyosi et al. The CYP3A1/2 enzyme is present at much higher levels in the brain mitochondrial fraction than in the microsomal fraction in contrast to what is observed in the liver. In general, there is limited availability data reported about isoforms of Cyp3a in rat brains. It can be challenging to predict CYP3A expression and activity. This is due to the low levels of CYPs expressed in the brain dictate that many studies fail to detect CYP protein.

Midazolam hydroxylation MM kinetics have been reported in rat brain microsomes, but not mitochondria (Devaraj et al, 2021). We observed that the kinetics of microsomal formation of 4-hydroxymidazolam in our study were relatively comparable to the previously published data. However, the formation rates of 1'-hydroxymidazolam in our study were significantly lower than the values were reported earlier. The variation in microsomal activity observed in 1'OH MDZ data could be due to methodological differences between the two studies. For example, in the current study, we used the BCA assay for the estimation of microsomal and mitochondrial protein levels, whereas in the previous study, the Bradford assay was used. Bradford is a convenient and simple assay; however, some of its disadvantages include the nonlinearity of its standard curve, and a significant protein-to-protein variation (Olson & Markwell, 2007). This results in greater error rates and coefficients of variation (CV) values when compared to BCA assays. One of the BCA protein assay's strengths is its low protein-to-protein variability. Also, it has the advantage of not interacting with as many contaminants and buffers components, particularly detergents (Olson & Markwell, 2007).

The current findings highlighted the fact that the activity and content of microsomes and mitochondria are varied. The results presented in the previous chapter provide an evidence that

there is a major difference between microsome and mitochondria with respect to the content and activity. In addition, these data show that the method is accurate and reproducible to quantitate the midazolam metabolites in brain microsome and mitochondria fractions.

4.1.2 Subcellular fraction purity

Some contamination will inevitably occur in the various subcellular fractions obtained during the differential centrifugation method. Therefore, we used VDAC1 as a mitochondrial marker and calreticulin as a microsomal marker. VDAC1 is used to determine the contamination of microsomes by mitochondria, and calreticulin is used to measure the contamination of mitochondria by microsomes. Based on the presence of VDAC1, as expected, the intensity of the antibody reactive bands was higher in mitochondrial proteins. These results suggest that mitochondrial preparation used in this study contains 19.3% contaminating microsomal fragments, which is a low but significant level of contamination. In addition, there was a 6.03% contamination with mitochondria in the microsomal samples, which is consistent with the previous study from our laboratory (DuBois *et al.*, 2019).

The cytochrome P450 (P450) enzymes are mostly found in the endoplasmic reticulum (ER), where they function as components of catalytic complexes that metabolize xenobiotics and some endogenous substrates. However, certain members of families CYP1–3 was discovered in additional subcellular compartments, including mitochondria. Although the physiological impact of this finding is unknown in the literature. Thus, it is critical to understand the molecular mechanisms by which P450s are targeted to these fractions.

CHAPTER 5

5.1 Conclusion

Studying CYP3A expression and activity in the brain is challenging because of the relatively low content of CYP activity in the brain and its regional localization. Despite this, CYP3A has been identified in microsome and mitochondria. The kinetics of midazolam activity in microsomal and mitochondrial fractions revealed a low affinity, high-capacity enzyme in the mitochondria with a V_{max} and K_m higher than in the brain microsomes.

In western blot analysis, the content of CYP3A protein was more intense in mitochondria compared to microsome. However, the affinity was higher in microsomal samples than mitochondrial fractions.

The ability of CYP3A enzymes in the brain to metabolize several endogenous and exogenous compounds suggests that they may affect the activity and fate of CNS drugs. However, the extent to which individual CYP3A isoforms contribute to this biotransformation remains to be elucidated. To optimize pharmacotherapy with such agents requires an understanding of the complex interplay between nuclear receptors in different regions of the brain and their ability to regulate the expression of CYP3A enzymes. Further studies of bio-transformed drugs by CYP3A enzymes in the brain are crucial to designing appropriate therapeutic strategies and preventing toxicity.

BIBLIOGRAPHY

- Abbott, N.J., 2005. Dynamics of CNS barriers: evolution, differentiation, and modulation. *Cell Mol Neurobiol* **25**, 5-23.
- Agarwal, V., Kommaddi, R.P., Valli, K., Ryder, D., Hyde, T.M., Kleinman, J.E., Strobel, H.W., Ravindranath, V., 2008. Drug metabolism in human brain: high levels of cytochrome P4503A43 in brain and metabolism of anti-anxiety drug alprazolam to its active metabolite. *PLoS One* **3**, e2337-e2337.
- Belloc, C., Baird, S., Cosme, J., Lecoeur, S., Gautier, J.C., Challine, D., de Waziers, I., Flinois, J.P., Beaune, P.H., 1996. Human cytochromes P450 expressed in *Escherichia coli*: production of specific antibodies. *Toxicology* **106**, 207-219.
- Bertz, R.J., Granneman, G.R., 1997. Use of in vitro and in vivo data to estimate the likelihood of metabolic pharmacokinetic interactions. *Clin Pharmacokinet* **32**, 210-258.
- Bibi, Z., 2008. Role of cytochrome P450 in drug interactions. *Nutrition & Metabolism* **5**, 27.
- Britto, M.R., Wedlund, P.J., 1992. Cytochrome P-450 in the brain. Potential evolutionary and therapeutic relevance of localization of drug-metabolizing enzymes. *Drug Metab Dispos* **20**, 446-450.
- Cederbaum, A.I., 2015. Molecular mechanisms of the microsomal mixed function oxidases and biological and pathological implications. *Redox Biol* **4**, 60-73.
- Chaobal, H.N., Kharasch, E.D., 2005. Single-point sampling for assessment of constitutive, induced, and inhibited cytochrome P450 3A activity with alfentanil or midazolam. *Clin Pharmacol Ther* **78**, 529-539.
- de Wildt, S.N., Kearns, G.L., Leeder, J.S., van den Anker, J.N., 1999. Cytochrome P450 3A: ontogeny and drug disposition. *Clin Pharmacokinet* **37**, 485-505.
- Venkatapura Chandrashekar, D., DuBois, B., & Mehvar, R., 2021. UPLC-MS/MS analysis of the Michaelis-Menten kinetics of CYP3A-mediated midazolam 1'- and 4-hydroxylation in rat brain microsomes. *Journal of Chromatography B*, 1180, 122892.
- Donato, M.T., Castell, J.V., 2003. Strategies and molecular probes to investigate the role of cytochrome P450 in drug metabolism: focus on in vitro studies. *Clin Pharmacokinet* **42**, 153-178.
- DuBois, B.N., Amirrad, F., Mehvar, R., 2019. Kinetics of dextromethorphan-O-demethylase activity and distribution of CYP2D in four commonly-used subcellular fractions of rat brain. *Xenobiotica* **49**, 1133-1142.
- Dutheil, F., Beaune, P., Lorient, M.A., 2008. Xenobiotic metabolizing enzymes in the central nervous system: Contribution of cytochrome P450 enzymes in normal and pathological human brain. *Biochimie* **90**, 426-436.
- Finnström, N., Bjelfman, C., Söderström, T.G., Smith, G., Egevad, L., Norlén, B.J., Wolf, C.R., Rane, A., 2001. Detection of cytochrome P450 mRNA transcripts in prostate samples by RT-PCR. *Eur J Clin Invest* **31**, 880-886.
- Fukasawa, T., Suzuki, A., Otani, K., 2007. Effects of genetic polymorphism of cytochrome P450 enzymes on the pharmacokinetics of benzodiazepines. *J Clin Pharm Ther* **32**, 333-341.

- Garfinkel, D., 2003. Studies on pig liver microsomes I. Enzymic and pigment composition of different microsomal fractions. *Arch Biochem Biophys* **409**, 7-15.
- Geick, A., Eichelbaum, M., Burk, O., 2001. Nuclear receptor response elements mediate induction of intestinal MDR1 by rifampin. *J Biol Chem* **276**, 14581-14587.
- Gervasini, G., Carrillo, J.A., Benitez, J., 2004. Potential role of cerebral cytochrome P450 in clinical pharmacokinetics: modulation by endogenous compounds. *Clin Pharmacokinet* **43**, 693-706.
- Ghosh, C., Gonzalez-Martinez, J., Hossain, M., Cucullo, L., Fazio, V., Janigro, D., Marchi, N., 2010. Pattern of P450 expression at the human blood-brain barrier: roles of epileptic condition and laminar flow. *Epilepsia* **51**, 1408-1417.
- Ghosh, C., Marchi, N., Desai, N.K., Puvenna, V., Hossain, M., Gonzalez-Martinez, J., Alexopoulos, A.V., Janigro, D., 2011. Cellular localization and functional significance of CYP3A4 in the human epileptic brain. *Epilepsia* **52**, 562-571.
- Guengerich, F.P., 1993. Cytochrome P450 Enzymes. *American Scientist* **81**, 440-447.
- Harding, B.W., Wong, S.H., Nelson, D.H., 1964. CARBON MONOXIDE-COMBINING SUBSTANCES IN RAT ADRENAL. *Biochim Biophys Acta* **92**, 415-417.
- Hedlund, E., Gustafsson, J.A., Warner, M., 2001. Cytochrome P450 in the brain; a review. *Curr Drug Metab* **2**, 245-263.
- Ingelman-Sundberg, M., 2004. Human drug metabolising cytochrome P450 enzymes: properties and polymorphisms. *Naunyn Schmiedebergs Arch Pharmacol* **369**, 89-104.
- Jabor, V.A., Coelho, E.B., Dos Santos, N.A., Bonato, P.S., Lanchote, V.L., 2005. A highly sensitive LC-MS-MS assay for analysis of midazolam and its major metabolite in human plasma: applications to drug metabolism. *J Chromatogr B Analyt Technol Biomed Life Sci* **822**, 27-32.
- Jancova, P., Anzenbacher, P., Anzenbacherova, E., 2010. Phase II drug metabolizing enzymes. *Biomed Pap Med Fac Univ Palacky Olomouc Czech Repub* **154**, 103-116.
- Jayyosi, Z., Cooper, K.O., Thomas, P.E., 1992. Brain cytochrome P450 and testosterone metabolism by rat brain subcellular fractions: presence of cytochrome P450 3A immunoreactive protein in rat brain mitochondria. *Arch Biochem Biophys* **298**, 265-270.
- Kahn, G.C., Rubenfield, M., Davies, D.S., Boobis, A.R., 1987. Phenacetin O-deethylase activity of the rat: strain differences and the effects of enzyme-inducing compounds. *Xenobiotica* **17**, 179-187.
- Kennedy, C.J., Tierney, K.B., 2012. Xenobiotic Protection/xenobioticprotection/Resistance Mechanisms in Organisms. In Meyers, R.A., (Ed.), *Encyclopedia of Sustainability Science and Technology*. Springer New York, New York, NY, pp. 12293-12314.
- Killer, N., Hock, M., Gehlhaus, M., Capetian, P., Knoth, R., Pantazis, G., Volk, B., Meyer, R.P., 2009. Modulation of androgen and estrogen receptor expression by antiepileptic drugs and steroids in hippocampus of patients with temporal lobe epilepsy. *Epilepsia* **50**, 1875-1890.
- Klingenberg, M., 1958. Pigments of rat liver microsomes. *Arch Biochem Biophys* **75**, 376-386.
- Koymans, L., Donn -op den Kelder, G.M., Koppele Te, J.M., Vermeulen, N.P., 1993. Cytochromes P450: their active-site structure and mechanism of oxidation. *Drug Metab Rev* **25**, 325-387.
- Krishna, D.R., Shekar, M.S., 2005. Cytochrome P450 3A: genetic polymorphisms and inter-ethnic differences. *Methods Find Exp Clin Pharmacol* **27**, 559-567.

- Kuban, W., Daniel, W.A., 2021. Cytochrome P450 expression and regulation in the brain. *Drug Metabolism Reviews* **53**, 1-29.
- Marchi, N., Hallene, K.L., Kight, K.M., Cucullo, L., Moddel, G., Bingaman, W., Dini, G., Vezzani, A., Janigro, D., 2004. Significance of MDR1 and multiple drug resistance in refractory human epileptic brain. *BMC Med* **2**, 37.
- Martignoni, M., Groothuis, G.M., de Kanter, R., 2006. Species differences between mouse, rat, dog, monkey and human CYP-mediated drug metabolism, inhibition and induction. *Expert Opin Drug Metab Toxicol* **2**, 875-894.
- Martinkova, E., Dontenwill, M., Frei, E., Stiborova, M., 2009. Cytotoxicity of and DNA adduct formation by ellipticine in human U87MG glioblastoma cancer cells. *Neuro Endocrinol Lett* **30 Suppl 1**, 60-66.
- McFadyen, M.C., Melvin, W.T., Murray, G.I., 2004. Cytochrome P450 enzymes: novel options for cancer therapeutics. *Mol Cancer Ther* **3**, 363-371.
- Mei, Q., Richards, K., Strong-Basalyga, K., Fauty, S.E., Taylor, A., Yamazaki, M., Prueksaritanont, T., Lin, J.H., Hochman, J., 2004. Using real-time quantitative TaqMan RT-PCR to evaluate the role of dexamethasone in gene regulation of rat P-glycoproteins *mdr1a/1b* and cytochrome P450 3A1/2. *J Pharm Sci* **93**, 2488-2496.
- Miksys, S.L., Tyndale, R.F., 2002. Drug-metabolizing cytochrome P450s in the brain. *J Psychiatry Neurosci* **27**, 406-415.
- Nelson, D.R., 2005. *Cytochrome P450: Structure, Mechanism, and Biochemistry*, 3rd ed Edited by Paul R. Ortiz de Montellano (University of California, San Francisco). Kluwer Academic/Plenum Publishers: New York. 2005. xx + 690 pp. \$149.00. ISBN 0-306-48324-6. *Journal of the American Chemical Society* **127**, 12147-12148.
- Nelson, D.R., Koymans, L., Kamataki, T., Stegeman, J.J., Feyereisen, R., Waxman, D.J., Waterman, M.R., Gotoh, O., Coon, M.J., Estabrook, R.W., Gunsalus, I.C., Nebert, D.W., 1996. P450 superfamily: update on new sequences, gene mapping, accession numbers and nomenclature. *Pharmacogenetics* **6**, 1-42.
- Omura, T., 1999. Forty years of cytochrome P450. *Biochem Biophys Res Commun* **266**, 690-698.
- Omura, T., Sato, R., 1964. THE CARBON MONOXIDE-BINDING PIGMENT OF LIVER MICROSOMES. I. EVIDENCE FOR ITS HEMOPROTEIN NATURE. *J Biol Chem* **239**, 2370-2378.
- Omura, T., Sato, R., Cooper, D.Y., Rosenthal, O., Estabrook, R.W., 1965. Function of cytochrome P-450 of microsomes. *Fed Proc* **24**, 1181-1189.
- Olson, B. J. S. C., & Markwell, J. (2007). Assays for determination of protein concentration. *Current Protocols in Protein Science*, 48(1).<https://doi.org/10.1002/0471140864.ps0304s48>
- Pai, H.V., Upadhyaya, S.C., Chinta, S.J., Hegde, S.N., Ravindranath, V., 2002. Differential metabolism of alprazolam by liver and brain cytochrome (P4503A) to pharmacologically active metabolite. *Pharmacogenomics J* **2**, 243-258.
- Paine, M.F., Hart, H.L., Ludington, S.S., Haining, R.L., Rettie, A.E., Zeldin, D.C., 2006. The human intestinal cytochrome P450 "pie". *Drug Metab Dispos* **34**, 880-886.
- Raunio, H., Hakkola, J., Pelkonen, O., 2005. Regulation of CYP3A genes in the human respiratory tract. *Chem Biol Interact* **151**, 53-62.

- Rosenbrock, H., Hagemeyer C. E., Singec I., Knoth R., and Volk B. (1999). Testosterone Metabolism in Rat Brain Is Differentially Enhanced By Phenytoin-Inducible Cytochrome P450 Isoforms. *J Neuroendocrinol* **11**, 597-604.
- Schilter, B., Omiecinski, C.J., 1993. Regional distribution and expression modulation of cytochrome P-450 and epoxide hydrolase mRNAs in the rat brain. *Mol Pharmacol* **44**, 990-996.
- Schuetz, J.D., Beach, D.L., Guzelian, P.S., 1994. Selective expression of cytochrome P450 CYP3A mRNAs in embryonic and adult human liver. *Pharmacogenetics* **4**, 11-20.
- Sikka, R., Magauran, B., Ulrich, A., Shannon, M., 2005. Bench to bedside: Pharmacogenomics, adverse drug interactions, and the cytochrome P450 system. *Acad Emerg Med* **12**, 1227-1235.
- Taniguchi, H., Imai, Y., Sato, R., 1984. Role of the electron transfer system in microsomal drug monooxygenase reaction catalyzed by cytochrome P-450. *Arch Biochem Biophys* **232**, 585-596.
- Poulos, T. L., Finzel, B. C., & Howard, A. J. (1987). High-resolution crystal structure of cytochrome p450cam. *Journal of Molecular Biology*, 195(3), 687–700.
[https://doi.org/10.1016/0022-2836\(87\)90190-2](https://doi.org/10.1016/0022-2836(87)90190-2)
- Venkatapura Chandrashekar, D., Mehvar, R., 2020. UPLC-MS/MS analysis of CYP1A-mediated ethoxyresorufin-O-deethylation activity in the rat kidney microsomes. *J Chromatogr B Analyt Technol Biomed Life Sci* **1153**, 122272.
- Voirol, P., Jonzier-Perey, M., Porchet, F., Reymond, M.J., Janzer, R.C., Bouras, C., Strobel, H.W., Kosel, M., Eap, C.B., Baumann, P., 2000. Cytochrome P-450 activities in human and rat brain microsomes. *Brain Res* **855**, 235-243.
- Wada, A., & Waterman, M. R. (1992). Identification by site-directed mutagenesis of two lysine residues in cholesterol side chain cleavage cytochrome P450 that are essential for adrenodoxin binding. *Journal of Biological Chemistry*, 267(32), 22877–22882.
[https://doi.org/10.1016/s0021-9258\(18\)50028-4](https://doi.org/10.1016/s0021-9258(18)50028-4)
- Wang, H., Kawashima, H., Strobel, H.W., 1996. cDNA cloning of a novel CYP3A from rat brain. *Biochem Biophys Res Commun* **221**, 157-162.
- Warner, M., Köhler, C., Hansson, T., Gustafsson, J.A., 1988. Regional distribution of cytochrome P-450 in the rat brain: spectral quantitation and contribution of P-450b,e, and P-450c,d. *J Neurochem* **50**, 1057-1065.
- Westlind-Johnsson, A., Malmebo, S., Johansson, A., Otter, C., Andersson, T.B., Johansson, I., Edwards, R.J., Boobis, A.R., Ingelman-Sundberg, M., 2003. Comparative analysis of CYP3A expression in human liver suggests only a minor role for CYP3A5 in drug metabolism. *Drug Metab Dispos* **31**, 755-761.
- White, D.L.N.M.P.M.D., 2017. Clinical chemistry.
- Wijnen, P.A., Op den Buijsch, R.A., Drent, M., Kuijpers, P.M., Neef, C., Bast, A., Bekers, O., Koek, G.H., 2007. Review article: The prevalence and clinical relevance of cytochrome P450 polymorphisms. *Aliment Pharmacol Ther* **26 Suppl 2**, 211-219.

- Woodland, C., Huang, T.T., Gryz, E., Bendayan, R., Fawcett, J.P., 2008. Expression, activity and regulation of CYP3A in human and rodent brain. *Drug Metab Rev* **40**, 149-168.
- Wrighton, S.A., Stevens, J.C., 1992. The human hepatic cytochromes P450 involved in drug metabolism. *Crit Rev Toxicol* **22**, 1-21.
- Yadav, S., Dhawan, A., Seth, P.K., Singh, R.L., Parmar, D., 2006. Cytochrome P4503A: evidence for mRNA expression and catalytic activity in rat brain. *Mol Cell Biochem* **287**, 91-99.